4. In wildlife and laboratory studies, BPA induces alteration in steroid biosynthesis/ metabolism/excretion.
5. Wildlife residing in sediment is likely exposed to higher levels of BPA.

4.2.3. Issue 3: Laboratory animal research—human exposure connection

1. Human exposure is likely to be continuous, unlike exposure in most laboratory animal studies of BPA pharmacokinetics.

4.2.4. Issue 4: Life stage—relationship to exposure pharmacokinetics and health effects

1. Clearance of BPA in the fetus is reduced compared to other life stages. Different effects and metabolic clearance mechanisms are also observed in neonatal and adult animals. Conjugation (glucuronidation) and other mechanisms of metabolic clearance of BPA thus vary throughout life.
2. Exposure to BPA during different life stages differentially influences reproductive cancer etiology and progression, and exposure during sensitive periods in organogenesis may increase susceptibility to development of cancers in some organs, such as the prostate and mammary glands.
3. Early life exposure to environmentally relevant BPA doses may result in persistent adverse effects in humans.
4. The function of the immune system can be altered following adult exposure to BPA.
5. Effects on insulin metabolism occur following adult exposure.

4.3. Areas of uncertainty and suggestions for future research

4.3.1. Issue 1: In vitro mechanistic research—laboratory animal research connection

1. Since BPA can act as an agonist or an antagonist in different tissues and against different background physiological states, the specific co-regulators that mediated these different responses of BPA need to be elucidated based on *in vitro* mechanistic studies, which should be confirmed *in vivo*.
2. Research is needed on specific receptor sub-types (i.e., classical nuclear and non-classical membrane-associated estrogen receptors) in relation to the potency of BPA in different tissues.
3. The identification of multiple estrogen receptor genes and variants as well as different co-regulators with different activities reveals that different levels of potency of BPA could be obtained by complex interactions between these different components that would not be predicted in homogeneous recombinant systems.

4.3.2. Issue 2: Wildlife—laboratory animal research connection

1. To directly relate the effects seen in wildlife with BPA exposure, biomonitoring data are needed from wildlife. In addition to BPA levels, these studies should assay total estrogenic and antiandrogenic activity from other contaminants.
2. There is a need to examine sensitive endpoints in wildlife that have been identified in laboratory animals.
3. There are substantial amounts of plastic debris within marine and fresh water ecosystems, and studies are needed to examine the impact of BPA in the environment on aquatic organisms. Doses used in laboratory experiments involving wildlife should reflect environmental exposures.
4. More studies need to be done with BPA in invertebrates, and a fundamental understanding of estrogen action in invertebrates is required.
5. Studies should determine if amplification of BPA through the food chain occurs, particularly under anaerobic or hypoxic conditions due to the lack of microbial or photodegradation.
6. Future research emphasis should be placed on populations of aquatic animals exposed to landfill leachate and sewage effluent, as these are the primary point sources for BPA exposure.

4.3.3. Issue 3: Laboratory animal research—human exposure connection

1. Even though there have been attempts to estimate daily human intake of BPA, these estimates require many assumptions. The best measures we have to estimate whether humans may be affected by current exposures to BPA are levels in blood (not exposure levels), which can be related to blood levels in experimental animals after acute exposures. Known sources of human exposure to BPA do not appear sufficient to explain levels measured in human tissues and fluids.
2. While BPA is not persistent in the environment or in humans, biomonitoring surveys indicate that exposure is continuous. This is problematic because acute animal exposure studies are used to estimate daily human exposure to BPA, and at this time, we are not aware of any studies that have examined BPA pharmacokinetics in animal models following continuous low level exposures. Measurement of BPA levels in serum and other body fluids suggests that either BPA intake is much higher than accounted for, or that BPA can bioaccumulate in some conditions such as pregnancy, or both. Research using both animal models, as well as epidemiology studies, are needed to address these hypotheses, and this research needs to better mimic the apparent continuous exposure of humans to BPA.
3. More comprehensive exposure and biomonitoring studies are needed, especially in developing countries.
4. In both animal and human studies, internal exposure measures need to be related to health effects. In particular, there is a need for epidemiological studies relating health outcomes to BPA exposure, particularly during sensitive periods in development. These studies should be based on hypotheses from findings in experimental animals. This will require additional development of appropriate biomarkers in animal studies that can be used in epidemiological research.

4.3.4. Issue 4: Life stage—relationship to exposure pharmacokinetics and health effects

1. While there is a great need to continue studying prenatal and perinatal exposures in laboratory animal studies, many organs and endpoints continue developing at later stages (throughout puberty and adolescence). Additional studies are needed during these later periods of development.
2. Additional research is needed regarding exposure to BPA in adulthood to determine whether post-exposure effects are temporary or are permanent and associated with subsequent age-related diseases.
3. Because aging adults lose repair mechanisms, metabolic enzymes, and imprinted genes, the possibility that adult exposures (long-term, low level) can increase the risk of cancers and other conditions during aging should be addressed with additional human research and the development of appropriate animal models.
4. Epigenetics should be examined as a potential mechanism mediating developmental effects as well as the trans-generational effects of BPA and other contaminants. Potential effects of adult exposures also need to be examined in relation to disruption of epigenetic changes that occur normally during aging.
5. Trans- and multi-generational effects of BPA must be examined in laboratory animals and humans.
6. There is a need for studies that involve collection of human blood and urine from humans at several life stages, with specific emphasis on infants and young children and continued monitoring throughout adulthood. Additionally, there is a need to characterize the basis for the variability in BPA levels in studies examining both human urine and serum.
7. There is a need for research on the genetic basis for differences in susceptibility to BPA and other contaminants.
8. Studies are needed on comparative BPA pharmacokinetics in invertebrates and vertebrates (non-human primates included).
9. There is a need to measure total endocrine disrupter load in humans and wildlife. Therefore, biomarkers of endocrine disrupter exposure are necessary.
10. There is a need for more research directed at examining human exposure, pharmacokinetics and health effects of selected BPA precursors (i.e., BADGE, BISGMA, and BISDMA) and metabolites (e.g., halogenated BPAs).
11. There is a need for more studies focused on identification of other (non-estrogen-receptor mediated) mechanisms of action of BPA.
12. Effects of chemicals on the immune system are life stage dependent, and identifying the life stage dependency for BPA effects on the immune system is necessary. In addition, studies examining BPA effects on the immune system in wildlife are necessary.

5. Conclusions

The published scientific literature on human and animal exposure to low doses of BPA in relation to *in vitro* mechanistic studies reveals that human exposure to BPA is within the range that is predicted to be biologically active in over 95% of people sampled. The wide range of adverse effects of low doses of BPA in laboratory animals exposed both during development and in adulthood is a great cause for concern with regard to the potential for similar adverse effects in humans. Recent trends in human diseases relate to adverse effects observed in experimental animals exposed to low doses of BPA. Specific examples include: the increase in prostate and breast cancer, uro-genital abnormalities in male babies, a decline in semen quality in men, early onset of puberty in girls, metabolic disorders including insulin resistant (type 2) diabetes and obesity, and neurobehavioral problems such as attention deficit hyperactivity disorder (ADHD).

There is extensive evidence that outcomes may not become apparent until long after BPA exposure during development has occurred. The issue of a very long latency for effects *in utero* to be observed is referred to as the developmental origins of adult health and disease (DOHaD) hypothesis. These developmental effects are irreversible and can occur due to low dose exposure during brief sensitive periods in development, even though no BPA may be detected when the damage or disease is expressed. However, this does not diminish our concern for adult exposure, where many adverse outcomes are observed while exposure is occurring. Concern regarding exposure throughout life is based on evidence that there is chronic, low level exposure of virtually everyone in developed countries to BPA. These findings indicate that acute studies in animals, particularly traditional toxicological studies that only involve the use of high doses of BPA, do not reflect the situation in humans.

The fact that very few epidemiological studies have been conducted to address the issue of the potential for BPA to impact human health is a concern, and more research is clearly needed. This also applies to wildlife, both aquatic and terrestrial. The formulation of hypotheses for the epidemiological and ecological studies can be greatly facilitated by the extensive evidence from laboratory animal studies, particularly when common mechanisms that could plausibly mediate the responses are known to be very similar in the laboratory animal models, wildlife and humans.

Acknowledgements

Meeting support was provided by NIEHS and NIDCR, NIH/DHHS, the US-EPA and Commonweal. We thank Paul French for assistance with the meeting in web site and Albert Kingman for advice during preparation of the manuscript. This manuscript does not reflect US-EPA, USGS or NIH agency policy. FvS is supported by NIH grant ES11283.

References

[1] Vandenberg LN, Hauser R, Marcus M, Olea N, Welshons WV. Human exposure to bisphenol A (BPA). Reprod Toxicol 2007;24:139–77.
[2] Wetherill YB, Akingbemi B, Kanno J, McLachlan JA, Nadal A, Sonnenschein C, et al. In vitro molecular mechanisms of bisphenol A action. Reprod Toxicol 2007;24:178–98.

[3] Richter CR, Birnbaum LS, Farabollini F, Newbold RR, Rubin BS, Talsness CE, et al. In vivo effects of bisphenol A in laboratory rodent studies. Reprod Toxicol 2007;24:199–224.
[4] Crain DA, Eriksen M, Iguchi T, Jobling S, Laufer H, LeBlanc GA, et al. An ecological assessment of bisphenol A: evidence from comparative biology. Reprod Toxicol 2007;24:225–39.
[5] Keri RA, Ho S-M, Hunt PA, Knudsen KE, Soto AM, Prins GS. An evaluation of evidence for the carcinogenic activity of bisphenol A. Reprod Toxicol 2007;24:240–52.
[6] NTP. Final Report of the Endocrine Disruptors Low Dose Peer Review Panel. Raleigh; NC. http://ntp.niehs.nih.gov/index.cfm?objectid=06F5CE98-E82F-8182-7FA81C02D3690D47ml; 2001 (Access data: June 8, 2007).
[7] IRIS. Bisphenol A (CASRN 80-05-7). US-EPA Integrated Risk Information System Substance File. http://www.epa.gov/iris/subst/0356.htm; 1988 (Access data: June 8, 2007).
[8] Nagel SC, vom Saal FS, Thayer KA, Dhar MG, Boechler M, Welshons WV. Relative binding affinity-serum modified access (RBA-SMA) assay predicts the relative *in vivo* bioactivity of the xenoestrogens bisphenol A and octylphenol. Environ Health Perspect 1997;105(1):70–6.
[9] Colerangle JB, Roy D. Profound effects of the weak environmental estrogen-like chemical bisphenol A on the growth of the mammary gland of Noble rats. J Steroid Biochem Mol Biol 1997;60(1–2):153–60.
[10] Steinmetz R, Brown NG, Allen DL, Bigsby RM, Ben-Jonathan N. The environmental estrogen bisphenol A stimulates prolactin release *in vitro* and *in vivo*. Endocrinol 1997;138(5):1780–6.
[11] Burridge E. Bisphenol A: product profile. Eur Chem News 2003:17.
[12] Olea N, Pulgar R, Perez P, Olea-Serrano F, Rivas A, Novillo-Fertrell A, et al. Estrogenicity of resin-based composites and sealants used in dentistry. Environ Health Perspect 1996;104(3):298–305.
[13] Moore C. Synthetic polymers in the marine environment: what we know, what we need to know, what can be done? In: Ragaini RC, editor. Proceedings of Conference: International Seminar on Nuclear War and Planetary Emergencies, 36th Session, Erice, Sicily, August 2006. Singapore: World Scientific Publishers; in press.
[14] Coors A, Jones PD, Giesy JP, Ratte HT. Removal of estrogenic activity from municipal waste landfill leachate assessed with a bioassay based on reporter gene expression. Environ Sci Technol 2003;37(15):3430–4.
[15] Kawagoshi Y, Fujita Y, Kishi I, Fukunaga I. Estrogenic chemicals and estrogenic activity in leachate from municipal waste landfill determined by yeast two-hybrid assay. J Environ Monit 2003;5(2):269–74.
[16] Rudel RA, Brody JG, Spengler JD, Vallarino J, Geno PW, Sun G, et al. Identification of selected hormonally active agents and animal mammary carcinogens in commercial and residential air and dust samples. J Air Waste Manage Assoc 2001;51:499–513.
[17] Dodds EC, Lawson W. Synthetic oestrogenic agents without the phenanthrene nucleus. Nature 1936;137:996.
[18] Welshons WV, Nagel SC, vom Saal FS. Large effects from small exposures. III. Endocrine mechanisms mediating effects of bisphenol A at levels of human exposure. Endocrinology 2006;147(Suppl. 6):S56–69.
[19] Quesada I, Fuentes E, Viso-Leon MC, Soria B, Ripoll C, Nadal A. Low doses of the endocrine disruptor bisphenol-A and the native hormone 17beta-estradiol rapidly activate transcription factor CREB. FASEB J 2002;16(12):1671–3.
[20] Walsh DE, Dockery P, Doolan CM. Estrogen receptor independent rapid non-genomic effects of environmental estrogens on $[CA^{2+}]_i$ in human breast cancer cells. Mol Cell Endocrinol 2005;230(1–2):23–30.
[21] Wozniak AL, Bulayeva NN, Watson CS. Xenoestrogens at picomolar to nanomolar concentrations trigger membrane estrogen receptor-a mediated Ca++ fluxes and prolactin release in GH3/B6 pituitary tumor cells. Environ Health Perspect 2005;113:431–9.
[22] Zsarnovszky A, Le HH, Wang HS, Belcher SM. Ontogeny of rapid estrogen-mediated extracellular signal-regulated kinase signaling in the rat cerebellar cortex: potent nongenomic agonist and endocrine disrupting activity of the xenoestrogen bisphenol A. Endocrinol 2005;146(12):5388–96.
[23] vom Saal FS, Welshons WV. Large effects from small exposures. II. The importance of positive controls in low-dose research on bisphenol A. Environ Res 2006;100:50–76.
[24] Welshons WV, Thayer KA, Judy BM, Taylor JA, Curran EM, vom Saal FS. Large effects from small exposures. I. Mechanisms for endocrine-disrupting chemicals with estrogenic activity. Environ Health Perspect 2003;111(8):994–1006.
[25] Ho SM, Tang WY, Belmonte de Frausto J, Prins GS. Developmental exposure to estradiol and bisphenol A increases susceptibility to prostate carcinogenesis and epigenetically regulates phosphodiesterase type 4 variant 4. Cancer Res 2006;66(11):5624–32.

Frederick S. vom Saal *
Division of Biological Sciences, University of Missouri-Columbia, 105 Lefevre Hall, Columbia, MO 65211, United States

Benson T. Akingbemi
Department of Anatomy, Physiology and Pharmacology, Auburn University, Auburn, AL 36849, United States

Scott M. Belcher
Department of Pharmacology and Cell Biophysics, Center for Environmental Genetics, University of Cincinnati, Cincinnati, OH 45267, United States

Linda S. Birnbaum
U.S. Environmental Protection Agency, Research Triangle Park, NC 27709, United States

D. Andrew Crain
Biology Department, Maryville College, Maryville, TN 37804, United States

Marcus Eriksen
Algalita Marine Research Foundation, Los Angeles, CA 90034, United States

Francesca Farabollini
Department of Physiology, University of Siena, 53100 Siena, Italy

Louis J. Guillette Jr.
Department of Zoology, University of Florida, Gainesville, FL 32611, United States

Russ Hauser
Department of Environmental Health, Harvard School of Public Health, Boston, MA 02115, United States

Jerrold J. Heindel
Division of Extramural Research and Training, National Institute of Environmental Health Sciences, Research Triangle Park, NC 27709, United States

Shuk-Mei Ho
Department of Environmental Health, University of Cincinnati Medical School, Cincinnati, OH 45267, United States

Patricia A. Hunt
School of Molecular Biosciences, Washington State University, Pullman, WA 99164, United States

Taisen Iguchi
National Institutes of Natural Science, Okazaki Institute For Integrative Bioscience Bioenvironmental Science, Okazaki, Aichi 444-8787, Japan

Susan Jobling
Department of Biological Sciences, Brunel University, Uxbridge, Middlesex, UK

Jun Kanno
Division of Cellular & Molecular Toxicology, National Institute of Health Sciences, Tokyo 158-8501, Japan

Ruth A. Keri
Department of Pharmacology, Case Western Reserve University School of Medicine, Cleveland, OH 44106, United States

Karen E. Knudsen
Department of Cell and Cancer Biology, University of Cincinnati College of Medicine, Cincinnati, OH 45267, United States

Hans Laufer
Department of Molecular and Cell Biology, University of Connecticut, Storrs, CT 06269, United States

Gerald A. LeBlanc
Department of Environmental and Molecular Toxicology, North Carolina State University, Raleigh, NC 27695, United States

Michele Marcus
Department of Epidemiology, Rollins School of Public Health, Emory University, Atlanta, GA 30322, United States

John A. McLachlan
Center for Bioenvironmental Research, Tulane and Xavier Universities, New Orleans, LA 70112, United States

John Peterson Myers
Environmental Health Sciences, Charlottesville, VA 22902, United States

Angel Nadal
Instituto de Bioingeniería, Universidad Miguel Hernández, Elche 03202, Alicante, Spain

Retha R. Newbold
Laboratory of Molecular Toxicology, National Institute of Environmental Health Sciences, Research Triangle Park, NC 27709, United States

Nicolas Olea
CIBERESP Hospital Clinico-University of Granada, 18071 Granada, Spain

Gail S. Prins
Department of Urology, University of Illinois at Chicago, Chicago, IL 60612, United States

Catherine A. Richter
USGS, Columbia Environmental Research Center, Columbia, MO 65201, United States

Beverly S. Rubin
Department of Anatomy and Cellular Biology, Tufts Medical School, Boston, MA 02111, United States

Carlos Sonnenschein
Department of Anatomy and Cellular Biology, Tufts University School of Medicine, Boston, MA 02111, United States

Ana M. Soto
Department of Anatomy and Cell Biology, Tufts University School of Medicine, Boston, MA 02111, United States

Chris E. Talsness
Charité University Medical School Berlin, Campus Benjamin Franklin, Institute of Clinical Pharmacology and Toxicology, Department of Toxicology, 14195 Berlin, Germany

John G. Vandenbergh
Department of Zoology, North Carolina State University, Raleigh, NC 27695, United States

Laura N. Vandenberg
Tufts University Sackler School of Graduate Biomedical Sciences, Boston, MA 02111, United States

Debby R. Walser-Kuntz
Carleton College, Department of Biology, Northfield, MN 55057, United States

Cheryl S. Watson
Biochemistry and Molecular Biology Department, University of Texas Medical Branch, Galveston, TX 77555, United States

Wade V. Welshons
Department of Biomedical Sciences, University of Missouri, Columbia, MO 65211, United States

Yelena Wetherill
Department of Epidemiology, Harvard School of Public Health, Boston, MA 02115, United States

R. Thomas Zoeller
Biology Department, University of Massachusetts, Amherst, MA 01003, United States

* Corresponding author. Tel.: +1 573 882 4367; fax: +1 573 884 5020.
E-mail address: vomsaalf@missouri.edu (F.S. vom Saal)

8 June 2007
Available online 27 July 2007

Aromatase Localization in Human Breast Cancer Tissues: Possible Interactions between Intratumoral Stromal and Parenchymal Cells

Yasuhiro Miki,[1] Takashi Suzuki,[1,3] Chika Tazawa,[1] Yuri Yamaguchi,[7] Kunio Kitada,[8] Seijiro Honma,[9] Takuya Moriya,[5] Hisashi Hirakawa,[6] Dean B. Evans,[10] Shin-ichi Hayashi,[4] Noriaki Ohuchi,[2] and Hironobu Sasano[1,5]

Departments of [1]Pathology and [2]Surgical Oncology, Tohoku University Graduate School of Medicine, Divisions of [3]Pathology and [4]Molecular Medical Technology, School of Medicine, Course of Health Sciences, Tohoku University, [5]Department of Pathology, Tohoku University Hospital, and [6]Department of Surgery, Tohoku Kosai Hospital, Sendai, Japan; [7]Research Institute for Clinical Oncology, Saitama Cancer Center, Saitama, Japan; [8]Pharmaceutical Technology Department, Chugai Pharmaceutical Co., Ltd., Shizuoka, Japan; [9]Research Development Department, Teizo Medical Co., Ltd., Kanagawa, Japan; and [10]Novartis Institutes for BioMedical Research Basel, Oncology Research, Basel, Switzerland

Abstract

Aromatase is a key enzyme in intratumoral estrogen production required for the production of estrogens through the conversion of serum androgens in postmenopausal breast cancer patients. There have been, however, controversies regarding the intratumoral localization of aromatase in human breast carcinoma tissues. Therefore, we have first examined the intratumoral localization of aromatase mRNA/protein in 19 breast carcinomas using laser capture microdissection/quantitative reverse transcription-PCR (RT-PCR) and immunohistochemistry. Aromatase mRNA and protein were detected in both intratumoral stromal and parenchymal cells in breast carcinoma tissues. Subsequent microarray expression profiling and clustering analyses, in addition to quantitative RT-PCR studies, showed a significant positive correlation between aromatase and estrogen-related receptor α mRNA expression in isolated carcinoma cells. We further examined an interaction between stromal cells isolated from human breast carcinoma tissues and breast carcinoma cell lines using a coculture system to study the biological characteristic of aromatase expression in carcinoma cells. Aromatase mRNA and enzyme activity and 17β-hydroxysteroid dehydrogenase type 1 mRNA in breast carcinoma cell lines, including MCF-7 and SK-BR-3 cells, were up-regulated in the presence of patient-derived 32N or 74T intratumoral stromal cells. The results from steroid conversion assays were also consistent with the findings above. The results of our study also showed that aromatase inhibitors were more effective in inhibiting aromatization induced by coculture in MCF-7 than that in stromal 32N. The examination of the localization of aromatase and its regulation, including the interactions existing between different cell types in human breast carcinoma tissues, may provide important information as to achieving better clinical response to aromatase inhibitors in breast cancer patients. [Cancer Res 2007;67(8):3945–54]

Requests for reprints: Hironobu Sasano, Department of Pathology, Tohoku University Graduate School of Medicine, 2-1 Seiryo-machi, Aoba-ku, Sendai, Miyagi-ken 980-8575, Japan. Phone: 81-22-717-8050; Fax: 81-22-717-8051; E-mail: hsasano@patholo2.med.tohoku.ac.jp.

doi:10.1158/0008-5472.CAN-06-3105

Introduction

Estrogens play important roles in the growth and invasion of estrogen-dependent human breast carcinomas. While postmenopausal women have low levels of circulating plasma estrogens, the local synthesis or intratumoral production of estrogens that takes place in breast carcinoma tissue itself can lead to higher estrogen levels in the tumor (1, 2). Intratumoral production of estrogens occurs as a result of aromatization of C19 steroids such as androstenedione and testosterone into estrogens, and this is catalyzed by the cytochrome P450 aromatase enzyme (3–5). Previously, the localization of aromatase has been mostly examined using immunohistochemistry with the reported results demonstrating the presence of aromatase protein predominantly in tumoral stromal cells and adipocytes of breast carcinoma tissues (6, 7). However, there have been controversies regarding the cellular localization of intratumoral aromatase with other studies demonstrating aromatase immunoreactivity in carcinoma or parenchymal as well as stromal cells of human breast carcinoma tissues (8, 9).

Aromatase expression is well known to be regulated by various transcriptional factors, including nuclear receptors and their putative ligands in several types of human cells and tissues (10, 11). Both interleukins, such as interleukin (IL)-1, IL-6 and IL-11 released from carcinoma, and/or inflammatory cells have been shown to potently induce aromatase expression in adipose fibroblast cells (12). However, the correlation between nuclear receptors and aromatase in parenchymal or carcinoma cells of breast carcinoma tissues has remained largely unknown. In addition, there have been no studies reported examining whether the factors released from human intratumoral stromal cells affect aromatase expression of breast carcinoma or parenchymal cells.

Intratumoral aromatase has been considered a viable clinical target for the treatment of estrogen receptor–positive postmenopausal breast cancer patients (13). However, routine evaluation methods for the detection of intratumoral aromatase expression in clinical specimens have not been established. Therefore, in this study, we have first examined the localization of aromatase mRNA in 19 breast carcinoma tissues using laser capture microdissection (LCM), together with quantitative reverse transcription-PCR (RT-PCR), and then examined their correlation with clinicopathologic parameters of the patients. The expression and localization of the aromatase protein were also confirmed by immunohistochemistry using the aromatase monoclonal antibody termed 677 (14, 15). Microarray expression profiling and clustering analyses were also done on both isolated carcinoma and stromal cells obtained from the 19 breast carcinoma cases to identify possible

aromatase-regulating nuclear receptors in human breast carcinoma cells. We then examined the possible effects of isolated stromal cells from breast carcinoma tissues on both aromatase enzymatic activity and mRNA transcripts in breast carcinoma cell lines. Cocultured intratumoral stromal 32N or 74T cells, established from breast carcinoma tissues by primary culture, were used to evaluate the potential effects of carcinoma/stromal cell interactions on aromatase expression and enzyme activity in the carcinoma cells. Effects of coculture of MCF-7 cells with stromal 32N cells on MCF-7 cell proliferation and the inhibitory effects of the aromatase inhibitors on cell proliferation were subsequently investigated to further characterize the biological features of aromatase function in carcinoma or parenchymal cells.

Materials and Methods

Patients and tissue preparation. A total of 42 specimens of invasive ductal carcinoma of the breast were obtained from Japanese female patients from 2002 to 2005 at the Department of Surgery, Tohoku University Hospital and Tohoku Kosai Hospital (Sendai, Japan). The number of subjects examined in each experiment were as follows: 19 cases [54.2 years (range, 37–86; SD, 12.9)] for LCM/quantitative RT-PCR (qPCR) to investigate aromatase localization, 23 cases [55.0 years (range, 36–74; SD, 10.7)] for LCM/microarray studies, and 11 cases [53.1 years (range, 36–77; SD, 10.1)] for LCM/qPCR to validate results of microarray analysis. Nonpathologic breast and adipose tissues adjacent to the carcinoma were also available for examination in 12 out of 23 cases used in LCM/microarray analysis. Relevant clinical data were retrieved from the review of the patient's files. The histologic grade of each specimen was independently evaluated by three of the authors (T. Suzuki, T. Moriya, and H. Sasano), based on the modified methods of Bloom and Richardson (16), according to Elston and Ellis (17). The ethics committees at Tohoku University School of Medicine and Tohoku Kosai Hospital approved the research protocols (2004-144, 2005-068, and 2006-042, respectively), with informed consent being obtained from these patients before surgery in each institution.

Immunohistochemistry. For immunohistochemistry of aromatase, sequential frozen tissues, also used in the LCM analyses, were taken to examine the correlation between mRNA and protein in individual cellular compartments of the breast cancer tissues.

The aromatase monoclonal antibody 677 was raised against native recombinantly expressed human aromatase protein, with details of its characterization and utilization for immunohistochemistry being previously reported by the authors (14, 15). Tissue sections were immunostained by a biotin-streptavidin method with Histofine kit (Nichirei Co. Ltd., Tokyo, Japan). Breast carcinomas tissues were rapidly embedded in Tissue-Tek optimal cutting temperature compound (Sakura Finetechnical Co., Ltd., Tokyo, Japan) and frozen materials sectioned at a thickness of 3 μm. The antigen-antibody complex was then visualized with 3.3′-diaminobenzidine solution and counterstained with hematoxylin. Evaluation of aromatase immunohistochemistry was done as previously reported using 10% formalin-fixed and paraffin-embedded tissue specimens (14). The approximate percentage of cells staining (proportion score) were classified into the following four groups: 0, <1%; 1, ~25%; 2, ~50%; and 3, >50% immunopositive cells. Relative intensity of aromatase immunopositive cells was classified as follows: 0, no immunoreactivity; 1, weak; 2, moderate; and 3, intense immunoreactivity. Aromatase immunoreactivity was evaluated as a total score composed of the proportion score + relative immunointensity score.

Other antibodies used in this study for characterizing clinicopathologic parameters of the cases are as follows: monoclonal antibodies: ERα (ER1D5; Immunotech S.A., Marseilles, France), progesterone receptor (MAB429; Chemicon International Inc., Temecula, CA), and Ki-67 (MIB1; DakoCytomation Co. Ltd., Kyoto, Japan); and rabbit polyclonal antibody: HER-2/*neu* (Ao485; DakoCytomation). The rabbit polyclonal antibody for 17β-HSD1, 17β-HSD5, and monoclonal antibody for steroid sulfatase (STS) were kindly provided by Dr. Poutanen (University of Oulu, Finland), Dr. Lu (Laval University Hospital Center, Québec, Canada) and Kyowa Hakko Kogyo Co., Ltd. (Tokyo, Japan), respectively. These antibodies were used for immunohistochemistry in 10% formalin-fixed and paraffin-embedded tissue specimens of the cases. To score estrogen receptor (ER), progesteron receptor (PR), and Ki-67, more than 1,000 carcinoma cells from each case were counted independently by the same three authors as described above (Y.Miki, T. Suzuki, and H. Sasano), and the percentage of immunoreactivity as a labeling index (LI) was subsequently determined. The cases with <10% ERα LI or PR LI were designated ER- or PR-negative breast carcinomas according to the report by Allred et al. (18). For scoring of HER-2/*neu*, 17β-HSD1, 17β-HSD5, and STS (19–22), two groups were tentatively identified (0, no immunoreactivity and 1, positive carcinoma cells).

Total RNA extraction from breast tissues and cDNA synthesis. Total RNA was carefully extracted from 12 breast carcinoma specimens from both carcinomas and adipose compartments of the breast cancers in addition to nonpathologic breast tissues adjacent to the carcinoma using the TRIzol method (Invitrogen Corporation, San Diego, CA). A reverse transcription kit (Superscript II Preamplification system; Invitrogen) was used in the synthesis of cDNA.

Real-time RT-PCR. Real-time PCR was carried out using the LightCycler System (Roche Diagnostics GmbH, Mannheim, Germany). The primer sequences of aromatase, *ERRα*, and *RPL13A* were shown previously (23). Primer sets of *GCNF, HNF-4α, VDR, TRβ, TR4, HSD17B1, HSD17B2, HSD17B3, HSD17B4,* and *HSD17B5* were designed using OLIGO Primer Analysis Software (Takara Bio Inc., Shiga, Japan). cDNAs of known concentrations for target genes and the housekeeping gene, ribosomal protein L13a *(RPL13A)* were used to generate standard curves for real-time quantitative PCR to determine the quantity of target cDNA transcripts. The mRNA level in each case was represented as a ratio of *RPL13A* (%; refs. 20, 21, 23).

Laser Capture Microdissection. Nineteen breast carcinoma cases were frozen-sectioned at a thickness of 8 μm. Approximately 5,000 cells were laser-transferred from the carcinoma cells and the intratumoral stromal cells under light microscopic examination. For LCM/microarray expression profiling, after initial recovery and resuspension of the RNA pellet, a DNase digestion was done for 2 h at 37°C using 10 units of DNase (GenHunter, Nashville, TN) in the presence of 10 units of RNase inhibitor (Invitrogen), followed by extraction and precipitation. The pellet was resuspended in 27 μL of RNase-free H_2O and used for high-density cDNA array analysis.

Microarray analysis in isolated carcinoma cells. Twenty-three breast carcinomas were available for examination of gene expression patterns using microarray analysis following isolation by laser capture microscopy. Total RNA was extracted from ~5,000 carcinoma cells prepared by LCM procedures as described above. Sample preparation and processing were done essentially as described in the Affymetrix GeneChip Expression Analysis Manual (Affymetrix, Inc., Santa Clara, CA), with the exception that the labeled cRNA samples were hybridized to the complete human U133 GeneChip set (Affymetrix), including 22,215 and 22,577 genes. Relative levels of gene expression were calculated by global normalization. All gene expression data were clustered, and results were visualized using GeneSpring 7.2 (Agilent Technologies, Inc., Santa Clara, CA).

In this study, we focused on nuclear receptors that may modulate aromatase expression in carcinoma cells. Out of 44,792 genes, 88 genes were selected from the gene expression profiling for further analysis by reference to the web database of Nuclear Receptor.[11] Each case of breast carcinoma was ordered according to the level of aromatase gene expression determined by microarray and clustering analysis between each gene. Data from these categories and aromatase were subjected to hierarchical clustering analysis and visualization using the Cluster and TreeView programs (Stanford University, Palo Alto, CA; ref. 24) to generate tree structures based on the degree of similarity, as well as matrices comparing the levels of expression of individual genes in each sample examined. In addition, we further examined the correlations between the levels of aromatase mRNA expression and seven genes that were most closely

[11] NucleaRDB (April 2005, release 5.0); http://www.receptors.org/NR/index.html.

associated with aromatase in carcinoma cells isolated by LCM from 11 cases of human breast carcinoma.

Breast cancer cell lines and culture conditions. Human breast carcinoma cell lines MCF-7, T-47D, ZR-75-1, and SK-BR-3 and the human choriocarcinoma cell line BeWo were provided from the Cell Resource Center for Biomedical Research, Tohoku University (Sendai, Japan). Human breast carcinoma cell lines MDA-MB-231 and MDA-MB-468 and mouse preadipocyte 3T3-L1 cells were purchased from the American Type Culture Collection (Manassas, VA). The MCF-7, T-47D, ZR-75-1, and 3T3-L1 cell lines were maintained in RPMI 1640 (Sigma-Aldrich Co., St. Louis, MO) or Leivobitz's L-15 medium (Invitrogen) for the MDA-MB-231 and MDA-MB-468 cells and supplemented with 10% fetal bovine serum (FBS; SAFC Biosciences, Lenexa, KS). BeWo placental cells were maintained in Ham's F12 medium (Invitrogen) supplemented with 15% FBS. Primary stromal cells employed in this study were designated 74T and 32N and were isolated using collagenase treatment from human breast carcinoma tissues (25) and maintained in RPMI 1640 with 10% FBS.

Coculture system. For physical separation of stromal and carcinoma cell lines, transwell cultures were established in six-well plates or 100-mm dishes using Transwell Permeable Supports (0.4 μm pore; Corning, Incorporated, New York, NY). MCF-7 and SK-BR-3 cells were cultured in transwell chambers in the absence or presence of 32N, 74T, and 3T3-L1 cells and were cultivated on the bottom of the plates or dishes. After 24 h of cultivation using this coculture system, carcinoma and stromal cells were separated, and each component was examined in the aromatization assay, estrogen production assays, or by real-time RT-PCR. The cells after coculture with other cells were designated with subscript CO (i.e., MCF-7_{CO}, $32N_{CO}$). After these assays, viable cells were counted by the trypan blue exclusion (TBE) assay, and the total RNA was extracted using the TRIzol method described above.

Aromatization assay. Several previous studies have shown that the aromatase enzyme activity and/or mRNA levels were low or not detectable in the breast carcinoma cells such as MCF-7 (26–29). Therefore, in this study, we employed 6α-methylandrost-4-ene-3,17-dione (MeAD) assay as a quantitative evaluation of aromatization activity (30). The conversion of MeAD, an androgen analogue, into estrogen analogue (6α-methylestradiol) by aromatase was shown to be highly specific, and an evaluation of accurate aromatase activity could become possible with the measurement of its estrogen analogue produced (30). From the results of comparative studies using rat ovary tissue, the quantitative limit of detection of the MeAD assay was approximately 2-fold higher than that of the ^{3}H-water release assay (data not shown).

The aromatization assay using MeAD was done as described previously (30). MeAD and 6α-methylestradiol (MeE2) were generously provided by Dr. Numazawa (Tohoku Pharmaceutical College, Sendai, Japan). Estradiol-3-pentafluorobenzyl-17β-methylpyridinium ether (E2-PFBY) was synthesized at Teizo Medical Co., Ltd. (Kanagawa, Japan). We used LC-MS–grade water, methanol, and acetonitrile for liquid chromatography–tandem mass spectrometry (LC-MS/MS). The LC-MS/MS devices and measurement conditions were as follows: an API 4000 electrospray ionization mass spectrometer (MDS SCIEX; Applied Biosystems (Foster City, CA)) was used. For high-performance liquid chromatography (HPLC), an Agilent 1100 chromatograph (Agilent Technologies) was employed. HTC PAL autosampler (CTC Analytics AG Industriestrasse, Zwingen, Switzerland) and an X Terra MS C18 column (3.5 μm, 2.1 × 150 mm) were employed. Measurement was done in the positive ion mode. For the quantification of MeE2-PFBY, we used a product ion (m/z 353.2) produced from a precursor ion (m/z 558.3). On the other hand, product ion of ^{13}C-E2-PFBY was m/z 109.9 produced from precursor ion at m/z 548.2. For the quantification of MeE2, after estrone, $^{13}C_4$ (Hayashi Pure Chemical Industries, Inc., Osaka, Japan) was added to the medium, and the mixture was mixed. The extract was dissolved in methanol and reduced with 1% $NaBH_4$. The sample was dried and treated with pentafluorobenzyl bromide under 0.8% KOH ethanol. Then, the reactive solution was diluted with purified water, and a derivative was extracted with ether. The sample was dried under reduced pressure and mixed with 2% 2-fluoro-1-methylpyridinium-*p*-toluenesulfonate/dichloromethane and 10% triethylamine. E2-PFBY derivative was eluted with 10% formic acid solution/acetonitrile (2, 8). The elution vehicle was removed under reduced pressure, dissolved in 0.1 mL of the mobile phase, and used as a sample for LC-MS/MS.

Estrogen production assays. MCF-7 and MCF-7_{CO} cells were incubated at 37°C in FBS-free RPMI 1640 containing 10 nmol/L of androstenedione or testosterone as substrates for 24 h. Concentrations of estrone and estradiol were evaluated by LC-MS/MS analysis (31). All the cells treated with substrates were counted by TBE assay. After addition of 100 pg of androstenedione-$^2H_7$ (C/D/N Isotope Inc., Quebec, Canada), estrone-$^{13}C_4$, and estradiol-$^{13}C_4$ (Hayashi Pure Chemical Industries) as internal standards, steroids were extracted with diethyl ether from the media. The separated organic layer was evaporated and then dissolved in picolinoic anhydride in

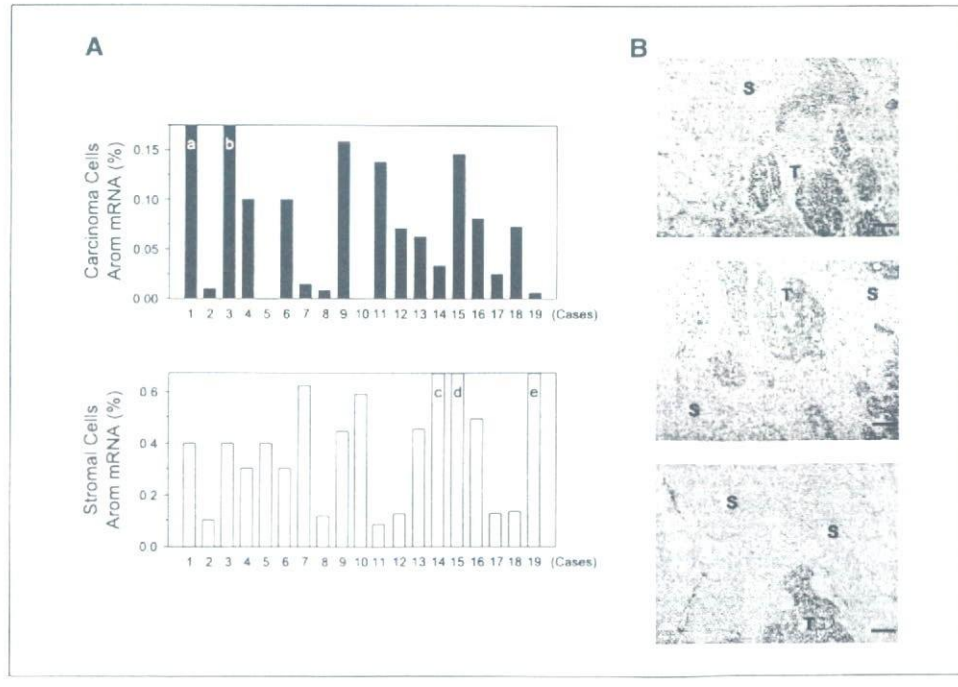

Figure 1. *A*, aromatase mRNA level in each case (1 to 19) of breast carcinoma (*top*) and stromal (*bottom*) cells. There were no detectable levels of aromatase in the breast carcinoma cells from two cases (5 and 10). For the following samples, the values of aromatase mRNA were *a* = 0.20%, *b* = 0.30%, *c* = 0.91%, *d* = 6.23%, and *e* = 1.02%. Aromatase immunoreactivity scores for each case (1 to 19) of breast carcinoma (*black*) and stromal (*white*) cells. There were no aromatase immunoreactivities observed in breast carcinoma cells from four cases (7, 12, 16, and 18). *B*, immunohistochemical localization of aromatase in human breast carcinoma tissues. Aromatase immunoreactivity was detected predominantly in carcinoma cells (*top*), only in stromal cells (*middle*), or in both carcinoma and stromal cells (*bottom*). *S*, stromal cells; *T*, carcinoma cells. *Bar*, 50 μm.

tetrahydrofran solution with triethylamine. After application to a Bond Elut C_{18} column, steroid derivatives were eluated with 80% acetonitrile solution. In this study, we used liquid chromatography (Agilent 1100; Agilent Technologies) coupled with an API 4000 triple-stage quadrupole mass spectrometer (Applied Biosystems) operated with electron spray isonization in the positive-ion mode, and the chromatographic separation was done on Cadenza CD-C_{18} columns (3 × 150 mm, 3.5 μm; Imtakt Corporation, Kyoto, Japan). Ion spray voltage was 4.5 kV, and turbo gas temperature was 450°C in ionization conditions. The estrogen levels in each case are presented as picograms per milliliter per 10^6 cells.

Cell proliferation assay. After coculture with stromal cells for 24 h, MCF-7 cells treated with 10^{-9} to 10^{-7} mol/L testosterone or androstenedione for 24 h were trypsinized and harvested in phenol red- and FBS-free medium in 96-well plates (3×10^4 cells/mL). Androstenedione and testosterone (10^{-9} to 10^{-7} mol/L) were added for 24 h. Cell proliferation was evaluated using the WST-8 method (Cell Counting Kit-8; Dojindo Inc., Kumamoto, Japan; ref. 32). We also examined the effects of aromatase inhibitors on cell proliferation by methods described above. Both steroidal (exemestane 10^{-8} mol/L; Pfizer Inc., New York, NY) and nonsteroidal (letrozole 10^{-8} mol/L; Novartis Pharma AG, Basel, Switzerland.) aromatase inhibitors were used in the androgen-treated MCF-7_{CO} and MCF-7 cells for 24 h.

Statistical analysis. Statistical analysis was done using the StatView 5.0 J software (SAS Institute Inc., Cary, NC). Values for patient's age, tumor size, Ki-67 LI, and mRNA levels for aromatase are represented as the mean ± SD. Simple regression analysis was employed to assess the correlations between aromatase and ERRα mRNA expression levels. An association between the degree of mRNA expression of aromatase and these parameters for each individual case was evaluated using one-way ANOVA and the Bonferroni test. Statistical differences between aromatase mRNA expression and ER status, PR status, menopausal status, stage, lymph node status, histologic grade and HER-2/*neu*, 17β-HSD1, and 17β-HSD5 immunoreactivities were all evaluated in a cross-table using the χ^2 test.

Results

Distributions of aromatase mRNA transcripts in breast tissues. The level of aromatase mRNA expression (mean ± SD; $n = 12$) was significantly higher in both carcinoma (1.327 ± 1.394%) and adipose tissues (2.103 ± 1.790%) than in non-neoplastic breast tissue (0.106 ± 0.095%) adjacent to carcinoma. The aromatase level in placenta tissues as a positive control was 80.770 ± 31.867% (mean ± SD; $n = 3$; data not shown).

Localization of intratumoral aromatase mRNA transcripts in breast carcinoma tissues. From 19 breast carcinoma cases, aromatase mRNA transcripts were detected in intratumoral stromal cells from all 19 cases and in the carcinoma cells from 17 of these cases (Fig. 1*A*). The mean value of aromatase mRNA transcript level was significantly higher ($P = 0.009$) in intratumoral stromal cells (0.348 ± 0.238) than in the carcinoma cells (0.112 ± 0.090). No significant correlation was detected in the aromatase mRNA level between stromal and carcinoma cells ($r = 0.132$, $P = 0.592$). Aromatase immunoreactivity was detected in the cytoplasmic compartment of both intratumoral stromal and carcinoma cells (Fig. 1*B* and *C*). Aromatase immunoreactivity was absent in the carcinoma cells of four cases.

Correlation between aromatase mRNA levels in intratumoral stromal and carcinoma cells and clinicopathologic status in breast carcinoma patients. An association between the intratumoral aromatase mRNA levels in stromal and/or parenchymal/carcinoma cells and clinicopathologic parameters in 19 breast carcinoma cases are summarized in Table 1. Two cases of aromatase-negative carcinoma cells were assigned as 0.000%. Aromatase mRNA levels in stromal cells were positively correlated with histologic grade ($P = 0.032$). Aromatase mRNA levels in

Table 1. Correlation between aromatase expression levels and clinicopathologic parameters in 19 breast carcinomas

Parameter	*n*	Carcinoma cells		Stromal cells	
		Mean ± SD	*P*	Mean ± SD	*P*
Histologic grade					
I + II	14	0.098 ± 0.085		0.342 ± 0.228	
III	5	0.014 ± 0.014	0.072	2.002 ± 2.847	0.032*
ER status					
+	11	0.116 ± 0.087		0.374 ± 0.239	
−	8	0.029 ± 0.031	0.015*	1.146 ± 2.080	0.234
PR status					
+	12	0.107 ± 0.089		0.337 ± 0.228	
−	7	0.033 ± 0.032	0.051	1.320 ± 2.190	0.134
17β-HSD1 status					
+	10	0.134 ± 0.090		0.413 ± 0.230	
−	9	0.028 ± 0.029	0.007*	1.101 ± 2.100	0.373
17β-HSD5 status					
+	11	0.096 ± 0.104		0.361 ± 0.164	
−	8	0.062 ± 0.052	0.437	1.266 ± 2.225	0.24
STS status					
+	12	0.074 ± 0.068		0.435 ± 0.292	
−	7	0.102 ± 0.135	0.592	1.723 ± 3.012	0.138
EST status					
+	8	0.068 ± 0.066		0.462 ± 0.337	
−	11	0.087 ± 0.094	0.683	0.891 ± 1.790	0.609

*Significantly different; in percent.

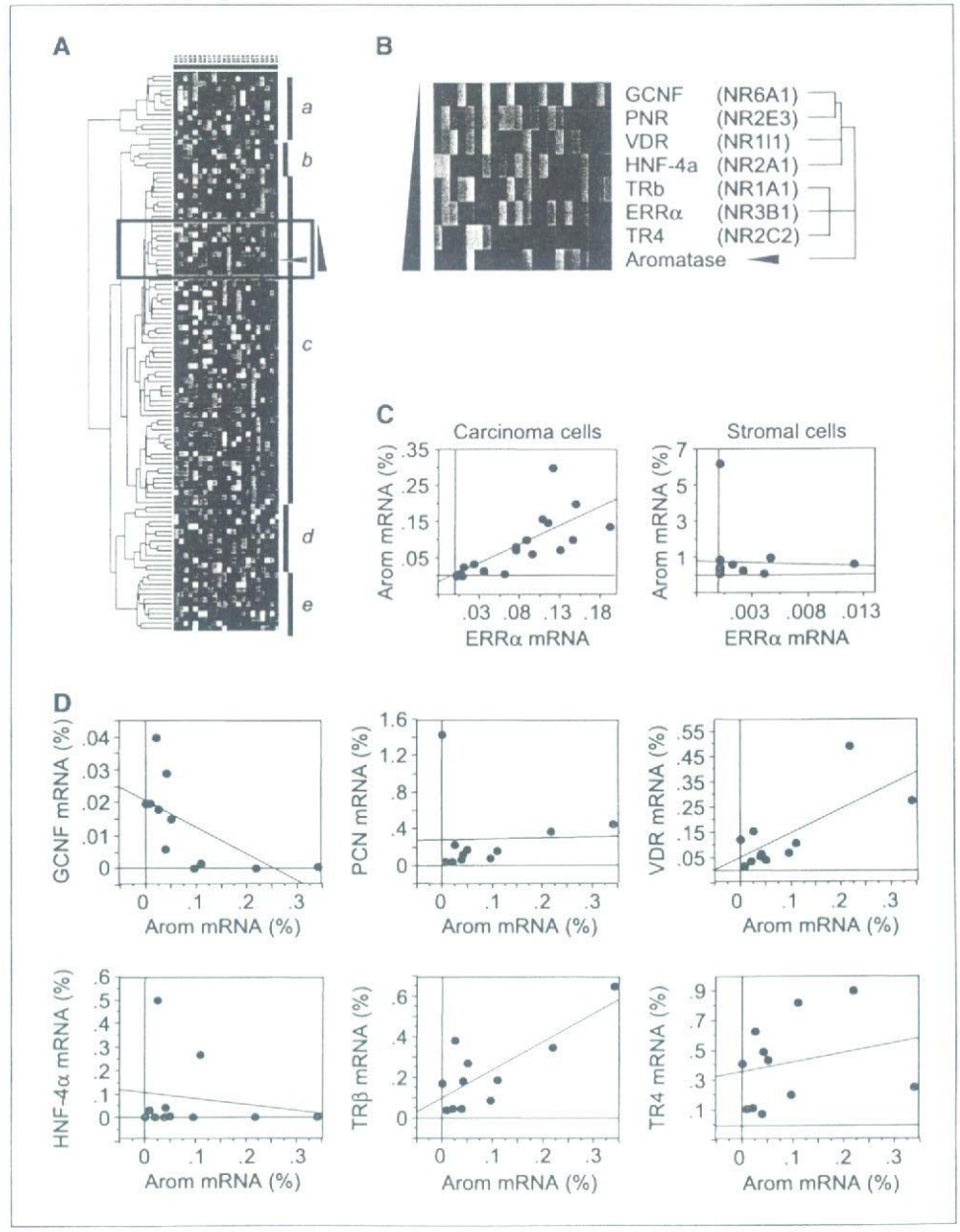

Figure 2. *A* and *B*, clustering analysis of microarray expression profiles of nuclear receptor genes. The cluster associated with the aromatase gene was composed of 59 genes (*A*, *group c*). More closely associated with the aromatase gene (*A*, *square*) were 12 genes (*B*). *C*, a statistically significant positive correlation was detected between aromatase and ERRα gene in 19 cases of (*left*) carcinoma cells ($r = 0.748$, $P = 0.002$), but not in (*right*) stromal cells ($r = 0.044$, $P = 0.860$). *D*, statistically significant correlations were detected between aromatase and ERRα ($r = 0.74$, $P = 0.01$; data not shown), VDR ($r = 0.73$, $P = 0.02$), TRβ ($r = 0.62$, $P = 0.04$), and GCNF ($r = -0.64$, $P = 0.03$) genes in 11 cases of carcinoma cells. No statistically significant correlations were detected between aromatase and PNR ($r = 0.02$, $P = 0.95$), HNF-4α ($r = -0.17$, $P = 0.61$), and TR4 ($r = 0.24$, $P = 0.48$) gene in 11 cases of carcinoma cells.

parenchymal/carcinoma cells were positively correlated with ER status ($P = 0.015$) and 17β-HSD1 status ($P = 0.007$), but not with histologic grade ($P = 0.072$). No significant association was detected between aromatase mRNA level in stromal or carcinoma cells and age, tumor size, lymph node status, PR status, HER-2/*neu* status, Ki-67 LI, 17β-HSD5 status, and STS status in this study.

Microarray analysis evaluated by hierarchical clustering. The results of focused clustering analysis subclassified 88 genes into five well-defined expression profiles or groups (Fig. 2*A*, *groups a–e*). The aromatase gene was included in group c (59 genes). The following seven genes were most closely associated with aromatase in group c (Fig. 2*B*): GCNF (NR6A1), PNR (NR2E3), VDR (NR1I1), HNF-4α (NR2A1), TRβ (NR1A1), ERRα (NR3B1), and TR4 (NR2C2).

Correlation between aromatase and nuclear receptors in isolated breast carcinoma cells. A statistically significant positive correlation was detected between aromatase and ERRα ($r = 0.74$, $P = 0.01$), VDR ($r = 0.73$, $P = 0.02$), and TRβ ($r = 0.62$, $P = 0.04$) in parenchymal/carcinoma cells of 11 human breast carcinoma cases (Fig. 2*D*). A statistically significant negative correlation was also detected between aromatase and GCNF ($r = -0.64$, $P = 0.03$) in these isolated parenchymal/carcinoma cells (Fig. 2*D*).

There were no significant increases or decreases of mRNA levels for the nuclear receptors GCNF, PNR, VDR, HNF-4α, TRβ, ERRα, and TR4 in MCF-7_{CO} compared with MCF-7 cells (data not present).

Correlation between aromatase and ERRα expressions in breast carcinoma cells. A statistically significant positive correlation was detected between aromatase and the ERRα gene (Fig. 2*C*) in 19 cases of parenchymal/carcinoma cells ($r = 0.748$, $P = 0.002$), but not in stromal cells ($r = 0.044$, $P = 0.860$).

In breast carcinoma cell lines, ERRα mRNA was detected in all cell lines examined in this study (Fig. 3*A*). Relatively low levels of

ERRα mRNA were detected in both stromal 32N and 74T cells. ERRα mRNA was also detected in placental BeWo cells.

Aromatase mRNA expression levels in human intratumoral stromal and carcinoma cells. Aromatase mRNA was detected in both stromal 32N and 74T cells isolated from human breast cancer tissues examined in this study, but the levels were lower than that of placental BeWo cells (Fig. 3*B*). Relatively low levels of aromatase mRNA was detected in mouse preadipocyte 3T3-L1 cells. Both 32N and 74T cells also exhibit aromatase enzyme activity, and there were no significant differences found between the aromatization levels in the 32N and 74T cells ($P = 0.140$).

Aromatase mRNA was detected in all breast carcinoma cell lines examined in this study (Fig. 3*B*). High levels of aromatase mRNA were detected in SK-BR-3 and MDA-MB-468 breast carcinoma cell lines, but the levels were lower than that of the 74T and 32N stromal cells and placental BeWo cells. We therefore used the higher aromatase mRNA expressing SK-BR-3 cells and the low aromatase mRNA expressing MCF-7 cells for further examinations. The aromatase mRNA level of native MCF-7 cells was significantly lower than that of native SK-BR-3 cells ($P = 0.041$). However, the levels in native SK-BR-3 cells were significantly lower than those of 32N ($P = 0.032$) or 74T cells ($P = 0.044$).

Effects of coculture on aromatase mRNA and activity levels in human intratumoral stromal and carcinoma cells. The results of the effects of coculture of breast cancer cell lines on the 32N and 74T cell aromatase activity are summarized in Fig. 3*C* to *E*. Aromatase mRNA level and activity in both 32N and 74T were significantly increased by cocultivation with MCF-7 but not with SK-BR-3 cells.

The results of the effects of coculture of stromal cells on MCF-7 and SK-BR-3 aromatase level are summarized in Fig. 3*D* and *E*. Both aromatase enzyme level (Fig. 3*D*) and mRNA level (Fig. 3*E*) in MCF-7_{CO} (after coculture with both 32N and 74T) were significantly higher than the levels found in monocultures of MCF-7 cells. There were no significant differences between native SK-BR-3 cells alone and SK-BR-3_{CO} (Fig. 3*D* and *E*). There were also no significant differences found in the aromatization levels between MCF-7_{CO} and SK-BR-3_{CO}. Aromatase activity/mRNA expression in both MCF-7_{CO} and 3T3-$L1_{CO}$, however, was not increased after coculture with MCF-7 and 3T3-L1 (Fig. 3*C–E*).

Effects of aromatase inhibitors on MCF-7 or stromal cells. Both 10^{-8} mol/L exemestane and 10^{-8} mol/L letrozole inhibited the increase in aromatization activity of the MCF-7_{CO} (Fig. 4*A*). Both 10^{-8} mol/L exemestane and 10^{-8} mol/L letrozole also inhibited the increase in aromatase activity of $32N_{CO}$ compared with the aromatase activity level of the 32N cells alone (Fig. 4*A*). The aromatization activity levels of MCF-7_{CO} following treatment with the aromatase inhibitors in MCF-7_{CO} were significantly lower than the aromatase activity level found in native MCF-7 cells (Fig. 4*A*).

The results of the cell proliferation assays are summarized in Fig. 4*B* to *D*. In monocultures of MCF-7 cells, there were no changes in the number of cells after 24 h incubation with 10^{-7} to 10^{-9} mol/L androstenedione, whereas 10^{-7} mol/L testosterone significantly increased the number of cells after 24 h. In MCF-7_{CO}, there were significant increments in the number of cells after 24 h treatment with 10^{-7} mol/L androstenedione and 10^{-8} to 10^{-7} mol/L testosterone. The cell numbers of MCF-7_{CO} treated with 10^{-8} mol/L androstenedione and 10^{-8} mol/L testosterone were significantly higher than those found in monocultures of MCF-7 cells. All of these increases of MCF-7_{CO} cell proliferation were inhibited following treatment with 10^{-8} mol/L exemestane (Fig. 4*C*) or 10^{-8} mol/L letrozole (Fig. 4*D*).

Estrogen production and expression levels of 17β-hydroxysteroid dehydrogenases in MCF-7. The results of estrogen production assays are summarized in Table 2*A* and *B*. Following the treatment with androstenedione (10^{-9} mol/L; 286.4 mg/mL) as the aromatase substrate, the rate of conversion into both estrone and estradiol in MCF-7_{CO} was higher than that in MCF-7 cells alone. The rate of conversion into estradiol but not into estrone in

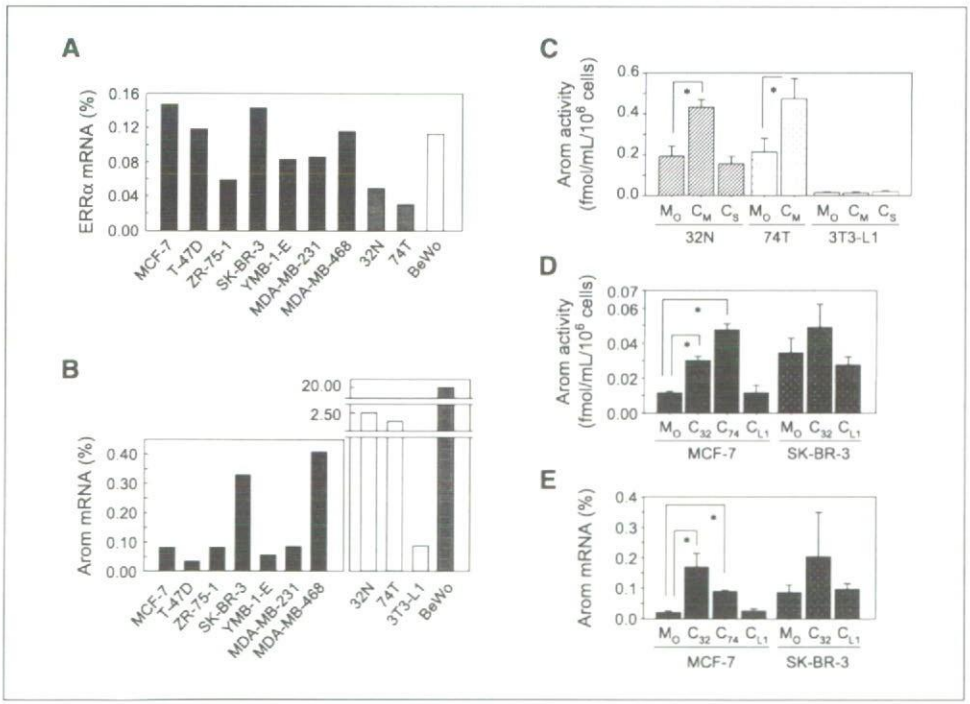

Figure 3. *A*, ERRα mRNA was detected in all breast carcinoma cell lines examined in this study, stromal 32N and 74T, and BeWo (in percent of RPL13A). *B*, aromatase levels in breast carcinoma cell lines and breast cancer-derived stromal 32N and 74T cells, mouse preadipocyte 3T3-L1 cells, and placental BeWo cells. *C–E*, the effects of coculture on aromatase mRNA level and enzyme activity in breast carcinoma and stromal cells. *C*, aromatase mRNA level in 32N, 74T, and 3T3-L1 cells; *D*, aromatase enzyme activity in MCF-7 and SK-BR-3 cells; *E*, aromatase mRNA level in MCF-7 or SK-BR-3 cells; M_O, monoculture; *C*, after coculture with 32N (C_{32}), 74T (C_{74}), 3T3-L1 (C_{L1}), MCF-7 (C_M), or SK-BR-3 (C_S) cells.

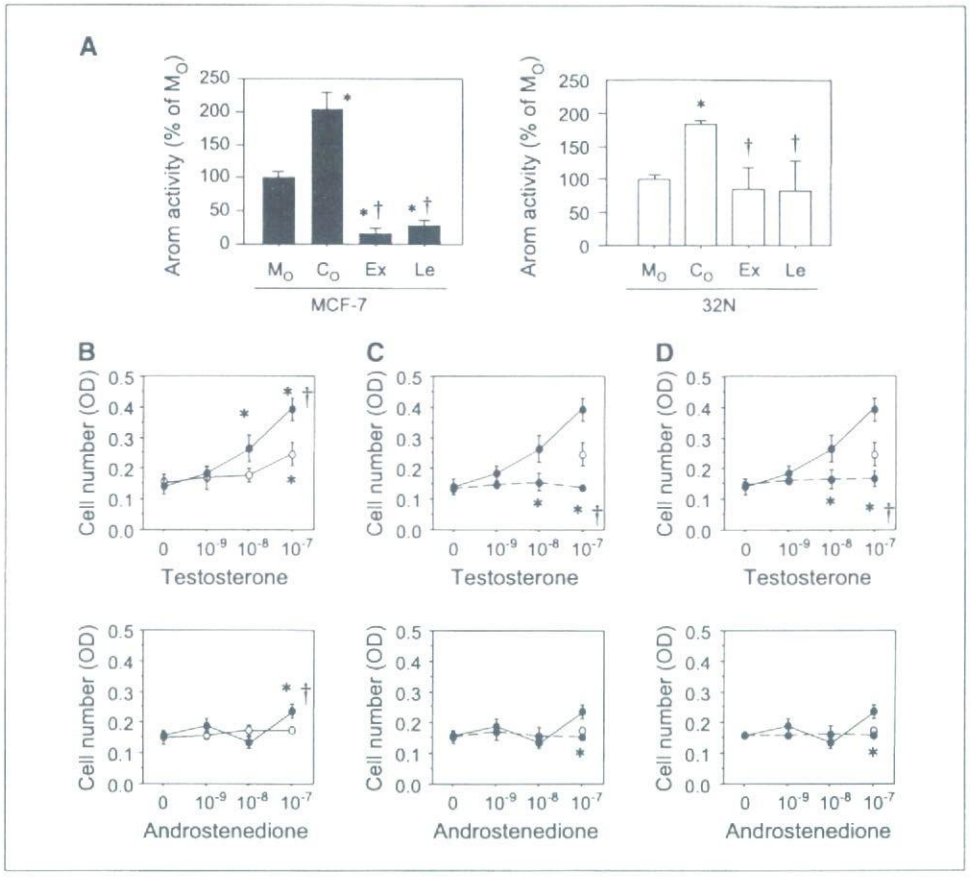

Figure 4. *A*, the effects of aromatase inhibitors on aromatase enzyme activities in MCF-7 (*left*) and 32N cells (*right*). *Ex*, treatment with 10^{-8} mol/L exemestane; *Le*, treatment with 10^{-8} mol/L letrozole; *, $P < 0.05$ versus M_O; †, $P < 0.05$ versus C_{32} C_{32} or C_M; in percent of RPL13A (aromatase mRNA level) or femtomoles per milliliter per 10^6 cells (aromatase enzyme activity). *B*, cell proliferation of $MCF\text{-}7_{CO}$ and MCF-7 cells treated with testosterone (*top*) and androstenedione (*bottom*). ●, $MCF\text{-}7_{CO}$; ○, MCF-7 cells; *, $P < 0.05$ versus vehicle control (0 nmol/L); †, $P < 0.05$ versus MCF-7 treated with 10 or 100 nmol/L androgens. *C* and *D*, cell proliferation following treatment with the aromatase inhibitors, (*C*) exemestane and (*D*) letrozole. ●, *solid line*, $MCF\text{-}7_{CO}$; ●, *dashed line*, $MCF\text{-}7_{CO}$ treated with aromatase inhibitor; ○, MCF-7; *, $P < 0.05$ versus $MCF\text{-}7_{CO}$; †, $P < 0.05$ versus MCF-7.

$MCF7_{CO}$ was also higher than that observed with MCF-7 cells alone, following the treatment with testosterone (10^{-9} mol/L; 288.4 mg/mL) as the aromatase substrate.

The results of 17β-hydroxysteroid dehydrogenases mRNA levels in cocultures and monocultures of MCF-7 cells are summarized in Table 2*C*. The 17β-HSD1 mRNA level in $MCF\text{-}7_{CO}$ was significantly higher than that found in MCF-7 cells. The 17β-HSD2 mRNA level in $MCF7_{CO}$ was significantly lower than that found in MCF-7 cells. There were no significant increases or decreases of other types of 17β-HSD types such as types 3, 4, and 5 in $MCF\text{-}7_{CO}$.

Discussion

Lu et al. (33) previously reported localization of aromatase protein and mRNA using immunohistochemistry and mRNA *in situ* hybridization, respectively, in the same breast cancer specimens. They showed that the aromatase protein and mRNA expression was predominantly detected in parenchymal cells (33). Further studies have shown the localization of aromatase protein using immunohistochemistry in human breast tissues (6–9), but the reported results have been markedly different between the different laboratories. These discrepancies in the cellular localization of intratumoral aromatase expression in human breast carcinomas may be due to the different aromatase antibodies and probe sequences employed in these different studies. This is the first study to show aromatase mRNA expression in the different cellular compartments of human breast carcinoma tissues following isolation using laser capture microscopy and subsequent qPCR analysis. The results of the combined LCM/qPCR study in our study showed that intratumoral aromatase in human breast cancer is expressed in both stromal and carcinoma or parenchymal components of the tissue. This finding confirms results of previous immunohistochemical study using the monoclonal antibody 677 done in 10% formalin-fixed and paraffin-embedded materials. We have also done immunohistochemistry using this monoclonal antibody 677 in frozen tissue sections adjacent to those in which LCM/qPCR analysis was conducted and have evaluated the immunoreactivity using the scoring system developed on 10% formalin-fixed and paraffin-embedded tissue specimens (14). Parenchymal/carcinoma cells are the major cell types of breast cancer tissues, and estrogens produced *in situ* by carcinoma cells could effectively activate the ER in the nuclei of carcinoma cells via an autocrine mechanism. Stromal cells also express aromatase, and thus, this source of intratumoral estrogen biosynthesis and subsequent estrogen-dependent cell proliferation is considered significant. An important aspect is the potential interplay that may exist between the carcinoma and stromal cell compartments. Therefore, we did further characterization of the potential regulation of aromatase in parenchymal or carcinoma cells in human breast cancer tissues.

Aromatase mRNA in adipose stromal cells was shown to be increased by coculture with MCF-7 cells (27). The results of previously reported studies all showed that various aromatase-stimulating factors (ASF), such as IL-1, IL-6, IL-11, IL-6 soluble receptor, tumor necrosis factor-α and prostaglandin E_2, etc. (10, 34, 35), are released from parenchymal or carcinoma cells, which resulted in the up-regulation of aromatase expression in stromal cells (including adipostromal cells, preadipocytes, or fibroblasts) within

Table 2.

(A) Estrogen production levels in MCF-7 and MCF-7_{CO}

Cells	Substrates	Concentrations*,†	
		E2	E1
MCF-7	AD	0.02	0.18
	TST	0.07	0.16
MCF-7_{CO}	AD	0.04	0.34
	TST	0.15	0.05

(B) Estrogen production ratios in MCF-7 and MCF-7_{CO}

Cells	Substrates	Conversion (%)*	
		AD→E1	TST→E2
MCF-7	AD	0.05	0.28
	TST	0.63	0.02
MCF-7_{CO}	AD	0.09	0.41
	TST	0.44	0.04

(C) mRNA levels of 17β-HSDs and 5α-reductases in MCF-7 and MCF-7_{CO} cells

Cells	mRNA levels (mean ± SD), %				
	HSD17B1	HSD17B2	HSD17B3	HSD17B4	HSD17B5
MCF-7	0.178 ± 0.076	0.040 ± 0.005	0.066 ± 0.114	0.016 ± 0.027	0.187 ± 0.091
MCF-7_{CO}	0.553 ± 0.047	0.009 ± 0.016	0.170 ± 0.061	0.014 ± 0.024	0.323 ± 0.172
P	0.047‡	0.030*	0.233	0.927	0.293

Abbreviations: AD, androstenedione; E2, estradiol; E1, estrone; TST, testosterone; MCF-7_{CO}, after coculture with 32N for 24 h.
*Mean of $n = 2$.
† In picograms per milliliter per 10^6 cells.
‡ Significant difference; $n = 3$; in percent of RPL13A.

human breast carcinoma tissues. Therefore, the possible effects of ASFs secreted from stromal cells on aromatase expression in parenchymal or carcinoma cells remained largely unknown possibly due to the reported low or no detectable aromatase enzyme levels of MCF-7 cells (26–29). Exogenous human epidermal growth factor (26), transforming growth factor (26), and keratinocyte growth factor (36) have all been reported to stimulate aromatase activity in MCF-7 cells. In our study, coculture of MCF-7 cells with stromal cells derived from human breast carcinoma tissues markedly induced the aromatase expression and activity in MCF-7 cells. Although we have not investigated which of the specific ASFs influence the expression of endogenous aromatase in MCF-7 cells, the ASFs described above could all be secreted from fibroblastic stromal cells adjacent to carcinoma, especially at the sites of stromal invasion, and have an influence. The precise ASFs involved would require further investigations to clarify their actual role.

The signals mediated through various nuclear receptors, including orphan nuclear receptors, have been postulated to influence aromatase activity and expression in breast carcinoma or parenchymal cells (10, 11, 37, 38). In our study, we showed that aromatase expression was closely associated with ERRα, VDR, GCNF, and TRβ expression in breast carcinoma cells. ERRα has been previously reported to be a positive regulator for aromatase gene expression in SK-BR-3 breast carcinoma cells (11), but not in the 3T3-L1 preadipocyte cells (39). ERRα is also known to bind to silencer elements located between promoter I.3 and II of the aromatase gene, which results in increased aromatase transcript levels in SK-BR-3 cells (11). The results of our study, including microarray expression profiling analyses, as well as those of a previously reported study (23), all showed that ERRα expression is positively correlated with aromatase expression in human breast carcinoma or parenchymal cells, but not with stromal cells or whole breast tissue containing both carcinoma and stromal cells (23). Therefore, ERRα is considered a key regulator of intratumoral estrogen production in human breast carcinoma or parenchymal cells, but not necessarily in stromal cells. However, there have been no studies reported on the possible correlations between aromatase gene expression and VDR, TRβ, or GCNF genes. VDR was well known as one of the estrogen target genes with an estrogen-responsive element in its promoter lesion (40). Therefore, the expression of VDR may be induced by estrogens synthesized by aromatase in human breast carcinoma cells. A statistically significant negative correlation was detected between aromatase and GCNF. GCNF was reported to be able to inhibit ERRα-mediated transactivation in human placental

choriocarcinoma cell lines (41). Therefore, GCNF may inhibit aromatase expression through the down-regulation of ERRα-mediated transactivation. The significance of TRβ expression in breast carcinoma cells has remained largely unknown. The mRNA levels of ERRα, TRβ, and GCNF in MCF-7 cells were, however, not increased following the coculture with stromal cells. Therefore, ASFs released from stromal cells may increase aromatase mRNA transcript levels through an interaction with these nuclear receptors above, but it awaits further investigations for clarification.

In the estrogen production assays, a relatively high rate of conversion into estradiol was detected in MCF-7_{CO}, but not MCF-7 cells alone following the treatment with testosterone as the aromatase substrate. Aromatase catalyzes testosterone into estradiol but not into estrone, whereas estrone is converted from androstenedione by aromatase (42). In our study, the level of estrone was decreased in MCF-7_{CO} compared with MCF-7 alone following the treatment with testosterone. Estrone is therefore considered to be converted from testosterone via androstenedione by 17β-HSD2. We also showed that the low level of 17β-HSD2 mRNA and the high level of 17β-HSD1 were detected in MCF-7_{CO}, but not MCF-7 alone. These findings all suggest that the rate of conversion into estrone in MCF-7_{CO} was lower than that in MCF-7 cells alone following the treatment with testosterone but not with androstenedione as the aromatase substrate. Interleukins were also shown to regulate 17β-HSDs mRNA and activity in human breast carcinoma cells (39, 43). Therefore, 17β-HSD1 expression may also be regulated by the factors released from stromal or carcinoma cells in addition to aromatase.

The coculture system used in our study could provided important information with regard to the evaluation of the intratumoral microenvironment such as cell-cell interactions and these soluble factors (44). It is also considered a useful model for examining the effect of medications on breast carcinoma patients. The adhesive microenvironment, including cell-matrix interactions and cell-cell interactions, plays an important role in the development of both the normal mammary gland and breast carcinoma (44). The results of our study also showed that aromatase inhibitors were more effective on aromatization increased by coculture of MCF-7 cells than in stromal 32N cells alone. These results suggest that the aromatase in parenchymal or carcinoma cells is the more important target for aromatase inhibitors in breast cancer patients because of the more effective decreases in aromatase activity in carcinoma cells. Therefore, it is clinically important to evaluate the localization of aromatase in breast carcinoma tissues to evaluate the possible efficacy of aromatase inhibitor treatment. However, it awaits further examinations to clarify all the interactions among the different cell types in human breast carcinomas.

Acknowledgments

Received 8/22/2006; revised 12/24/2006; accepted 2/2/2007.

Grant support: The Yasuda Medical Research Foundation, Osaka, Japan.

The costs of publication of this article were defrayed in part by the payment of page charges. This article must therefore be hereby marked *advertisement* in accordance with 18 U.S.C. Section 1734 solely to indicate this fact.

We thank Katsuhiko Ono and Toshie Suzuki (Department of Pathology, Tohoku University School of Medicine, Sendai, Japan) for skillful technical assistances.

References

1. Thorsen T, Tangen M, Stoa KF. Concentration of endogenous oestradiol as related to oestradiol receptor sites in breast tumor cytosol. Eur J Cancer Clin Oncol 1982;18:333–7.
2. van Landeghem AA, Poortman J, Nabuurs M, Thijssen JH. Endogenous concentration and subcellular distribution of estrogens in normal and malignant human breast tissue. Cancer Res 1985;45:2900–6.
3. Miller WR, Anderson TJ, Jack WJ. Relationship between tumour aromatase activity, tumour characteristics and response to therapy. J Steroid Biochem Mol Biol 1990;37:1055–9.
4. O'Neill JS, Elton RA, Miller WR. Aromatase activity in adipose tissue from breast quadrants: a link with tumour site. Br Med J (Clin Res Ed) 1988;296:741–3.
5. Bulun SE, Price TM, Aitken J, Mahendroo MS, Simpson ER. A link between breast cancer and local estrogen biosynthesis suggested by quantification of breast adipose tissue aromatase cytochrome P450 transcripts using competitive polymerase chain reaction after reverse transcription. J Clin Endocrinol Metab 1993;77:1622–8.
6. Sasano H, Nagura H, Harada N, Goukon Y, Kimura M. Immunolocalization of aromatase and other steroidogenic enzymes in human breast disorders. Hum Pathol 1994;25:530–5.
7. Santen RJ, Martel J, Hoagland M, et al. Stromal spindle cells contain aromatase in human breast tumors. J Clin Endocrinol Metab 1994;79:627–32.
8. Shenton KC, Dowsett M, Lu Q, et al. Comparison of biochemical aromatase activity with aromatase immunohistochemistry in human breast carcinomas. Breast Cancer Res Treat 1998;49:S101–7.
9. Brodie AM, Lu Q, Long BJ, et al. Aromatase and COX-2 expression in human breast cancers. J Steroid Biochem Mol Biol 2001;79:41–7.
10. Zhou J, Suzuki T, Kovacic A, et al. Interactions between prostaglandin E(2), liver receptor homologue-1, and aromatase in breast cancer. Cancer Res 2005;65:657–63.
11. Yang C, Zhou D, Chen S. Modulation of aromatase expression in the breast tissue by ERR α-1 orphan receptor. Cancer Res 1998;58:5695–700.
12. Simpson ER, Davis SR. Minireview: aromatase and the regulation of estrogen biosynthesis—some new perspectives. Endocrinology 2001;142:4589–94.
13. Smith IE, Dowsett M. Aromatase inhibitors in breast cancer. N Engl J Med 2003;348:2431–42.
14. Sasano H, Anderson TJ, Silverberg SG, et al. The validation of new aromatase monoclonal antibodies for immunohistochemistry—a correlation with biochemical activities in 46 cases of breast cancer. J Steroid Biochem Mol Biol 2005;95:35–9.
15. Cunat S, Rabenoelina F, Daures JP, et al. Aromatase expression in ovarian epithelial cancers. J Steroid Biochem Mol Biol 2005;93:15–24.
16. Bloom HJG, Richardson WW. Histological grading and prognosis in breast cancer. A study of 1409 cases of which 359 have been followed for 15 years. Br J Cancer 1957;11:359–77.
17. Elston CW, Ellis IO. Pathological prognostic factors in breast cancer. I. The value of histological grade in breast cancer. Expression from a large study with long-term follow-up. Histopathology 1991;19:403–10.
18. Allred DC, Harvey JM, Berardo M, Clark GM. Prognostic and predictive factors in breast cancer by immunohistochemical analysis. Mod Pathol 1998;11:155–68.
19. Miki Y, Nakata T, Suzuki T, et al. Systemic distribution of steroid sulfatase and estrogen sulfotransferase in human adult and fetal tissues. J Clin Endocrinol Metab 2002;87:5760–8.
20. Suzuki T, Nakata T, Miki Y, et al. Estrogen sulfotransferase and steroid sulfatase in human breast carcinoma. Cancer Res 2003;63:2762–70.
21. Suzuki T, Moriya T, Ariga N, Kaneko C, Kanazawa M, Sasano H. 17β-Hydroxysteroid dehydrogenase type 1 and type 2 in human breast carcinoma: a correlation to clinicopathological parameters. Br J Cancer 2000;82:518–23.
22. Suzuki T, Darnel AD, Akahira JI, et al. 5α-Reductases in human breast carcinoma: possible modulator of *in situ* androgenic actions. J Clin Endocrinol Metab 2001;86:2250–7.
23. Suzuki T, Miki Y, Moriya T, et al. Estrogen-related receptor α in human breast carcinoma as a potent prognostic factor. Cancer Res 2004;64:4670–6.
24. Eisen MB, Spellman PT, Brown PO, Botstein D. Cluster analysis and display of genome-wide expression patterns. Proc Natl Acad Sci U S A 1998;95:14863–8.
25. Yamaguchi Y, Takei H, Suemasu K, et al. Tumor-stromal interaction through the estrogen-signaling pathway in human breast cancer. Cancer Res 2005;65:4653–62.
26. Ryde CM, Nicholls JE, Dowsett M. Steroid and growth factor modulation of aromatase activity in MCF7 and T47D breast carcinoma cell lines. Cancer Res 1992;52:1411–5.
27. Harada N, Honda S. Molecular analysis of aberrant expression of aromatase in breast cancer tissues. Breast Cancer Res Treat 1998;49:S15–21.
28. Sanderson JT, Letcher RJ, Heneweer M, Giesy JP, van den Berg M. Effects of chloro-*s*-triazine herbicides and metabolites on aromatase activity in various human cell lines and on vitellogenin production in male carp hepatocytes. Environ Health Perspect 2001;109:1027–31.
29. Heneweer M, Muusse M, Dingemans M, de Jong PC, van den Berg M, Sanderson JT. Co-culture of primary human mammary fibroblasts and MCF-7 cells as an *in vitro* breast cancer model. Toxicol Sci 2005;83:257–63.
30. Numazawa M, Yoshimura A, Oshibe M. Enzymic aromatization of 6-alkyl-substituted androgens, potent competitive and mechanism-based inhibitors of aromatase. Biochem J 1998;329:151–6.
31. Suzuki T, Miki Y, Moriya T, et al. 5α-Reductase type 1 and aromatase in breast carcinoma as regulators of *in situ* androgen production. Int J Cancer 2007;120:285–91.

32. Miki Y, Suzuki T, Tazawa C, Ishizuka M, Semba S, Gorai I, Sasano H. Analysis of gene expression induced by diethylstilbestrol (DES) in human primitive Mullerian duct cells using microarray. Cancer Lett 2005;220:197–210.
33. Lu Q, Nakmura J, Savinov A, et al. Expression of aromatase protein and messenger ribonucleic acid in tumor epithelial cells and evidence of functional significance of locally produced estrogen in human breast cancers. Endocrinology 1996;137:3061–8.
34. Singh A, Purohit A, Wang DY, Duncan LJ, Ghilchik MW, Reed MJ. IL-6sR: release from MCF-7 breast cancer cells and role in regulating peripheral oestrogen synthesis. J Endocrinol 1995;147:R9–12.
35. Zhao Y, Agarwal VR, Mendelson CR, Simpson ER. Estrogen biosynthesis proximal to a breast tumor is stimulated by PGE2 via cyclic AMP, leading to activation of promoter II of the CYP19 (aromatase) gene. Endocrinology 1996;137:5739–42.
36. Zhang Y, Kulp SK, Sugimoto Y, Farrar WB, Brueggemeier RW, Lin YC. Keratinocyte growth factor (KGF) induces aromatase activity in cultured MCF-7 human breast cancer cells. Anticancer Res 1998;18:2541–6.
37. Mu YM, Yanase T, Nishi Y, Hirase N, Goto K, Takayanagi R, Nawata H. A nuclear receptor system constituted by RAR and RXR induces aromatase activity in MCF-7 human breast cancer cells. Mol Cell Endocrinol 2000;166:137–45.
38. Clyne CD, Speed CJ, Zhou J, Simpson ER. Liver receptor homologue-1 (LRH-1) regulates expression of aromatase in preadipocytes. J Biol Chem 2002;277:20591–7.
39. Simard J, Gingras S. Crucial role of cytokines in sex steroid formation in normal and tumoral tissues. Mol Cell Endocrinol 2001;171:25–40.
40. Bourdeau V, Deschenes J, Metivier R, et al. Genome-wide identification of high-affinity estrogen response elements in human and mouse. Mol Endocrinol 2004;18:1411–27.
41. Mehta DV, Kim YS, Dixon D, Jetten AM. Characterization of the expression of the retinoid-related, testis-associated receptor (RTR) in trophoblasts. Placenta 2002;23:281–7.
42. Suzuki T, Miki Y, Nakamura Y, et al. Sex steroid-producing enzymes in human breast cancer. Endocr Relat Cancer 2005;12:701–20.
43. Speirs V, Green AR, Atkin SL. Activity and gene expression of 17β-hydroxysteroid dehydrogenase type I in primary cultures of epithelial and stromal cells derived from normal and tumourous human breast tissue: the role of IL-8. J Steroid Biochem Mol Biol 1998;67:267–74.
44. Pirone DM, Chen CS. Strategies for engineering the adhesive microenvironment. J Mammary Gland Biol Neoplasia 2004;9:405–17.

ELSEVIER

Bone 40 (2007) 876–887

BONE

www.elsevier.com/locate/bone

Effects of aromatase inhibitors on human osteoblast and osteoblast-like cells: A possible androgenic bone protective effects induced by exemestane

Yasuhiro Miki [a], Takashi Suzuki [a], Masahito Hatori [b], Katsuhide Igarashi [c], Ken-ich Aisaki [c], Jun Kanno [c], Yasuhiro Nakamura [a], Miwa Uzuki [d], Takashi Sawai [c], Hironobu Sasano [a,*]

[a] *Department of Pathology, Tohoku University Graduate School of Medicine, 2-1 Seiryo-machi, Aoba-ku, Sendai, Miyagi, 980-8575, Japan*
[b] *Department of Orthopedic Surgery, Tohoku University Graduate School of Medicine, Sendai, Japan*
[c] *Division of Toxicology, National Institute of Health Sciences, Biological Safety Research Center, Setagaya, Tokyo, Japan*
[d] *Department of Pathology, Iwate Medical College, Morioka, Japan*

Received 21 April 2006; revised 6 November 2006; accepted 14 November 2006
Available online 28 December 2006

Abstract

Effects of aromatase inhibitors (AIs) on the human skeletal system due to systemic estrogen depletion are becoming clinically important due to their increasing use as an adjuvant therapy in postmenopausal women with breast cancer. However, possible effects of AIs on human bone cells have remained largely unknown. We therefore studied effects of AIs including the steroidal AI, exemestane (EXE), and non-steroidal AIs, Aromatase Inhibitor I (AI-I) and aminoglutethimide (AGM), on a human osteoblast. We employed a human osteoblast cell line, hFOB, which maintains relatively physiological status of estrogen and androgen pathways of human osteoblasts, i.e., expression of aromatase, androgen receptor (AR), and estrogen receptor (ER) β. We also employed osteoblast-like cell lines, Saos-2 and MG-63 which expressed aromatase, AR, and ERα/β in order to further evaluate the mechanisms of effects of AIs on osteoblasts. There was a significant increment in the number of the cells following 72 h treatment with EXE in hFOB and Saos-2 but not in MG-63, in which the level of AR mRNA was lower than that in hFOB and Saos-2. Alkaline phosphatase activity was also increased by EXE treatment in hFOB and Saos-2. Pretreatment with the AR blocker, flutamide, partially inhibited the effect of EXE. AI-I exerted no effects on osteoblast cell proliferation and AGM diminished the number of the cells. hFOB converted androstenedione into E2 and testosterone (TST). Both EXE and AI-I decreased E2 level and increased TST level. In a microarray analysis, gene profile patterns following treatment with EXE demonstrated similar patterns as with DHT but not with E2 treatment. The genes induced by EXE treatment were related to cell proliferation, differentiation which includes genes encoding cytoskeleton proteins. We also examined the expression levels of these genes using quantitative RT-PCR in hFOB and Saos-2 treated with EXE and DHT and with/without flutamide. HOXD11 gene known as bone morphogenesis factor and osteoblast growth-related genes were induced by EXE treatment as well as DHT treatment in both hFOB and Saos-2. These results indicated that the steroidal aromatase inhibitor, EXE, stimulated hFOB cell proliferation via both AR dependent and independent pathways.

Keywords: Osteoblast; Aromatase inhibitor; Androgen; Estrogen; Exemestane

Introduction

Results in various epidemiological or clinical studies demonstrated that estrogens play important protective roles in human skeletal as well as cardiovascular systems, and estrogen deficiency resulted in accelerating the development of osteoporosis in postmenopausal women [1–3]. In breast cancer of postmenopausal women, hormone therapies without any clinically deleterious effects due to estrogen deficiency on bone metabolism as well as lipid metabolisms are preferable. Estrogen deficiency has been generally detected in the patients with breast cancer following chemotherapy induced ovarian failure, gonadotropin analogue, and aromatase inhibitors (AIs) therapy [4]. Aromatase is the pivotal enzyme of *in situ* or intratumoral estrogen biosynthesis in postmenopausal breast cancer patients, and catalyzes the conversion from androgens into estrogens (Fig. 1A). AIs therefore play an important role in

* Corresponding author. Fax: +81 22 273 5976.
E-mail address: hsasano@patholo2.med.tohoku.ac.jp (H. Sasano).

8756-3282/$ - see front matter © 2006 Elsevier Inc. All rights reserved.
doi:10.1016/j.bone.2006.11.029

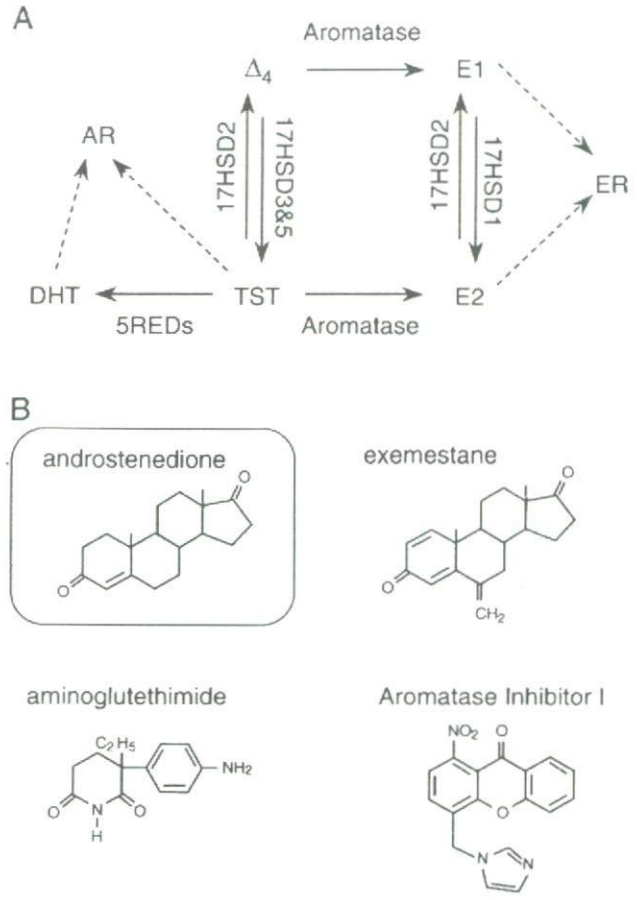

Fig. 1. (A) Summary of the pathway of estrogens and androgens production. Aromatase catalyzes the change from androstenedione (Δ4) and testosterone (TST) into estrone (E1) and estradiol (E2), respectively. 17HSD, 17β-hydroxysteroid dehydrogenase; 5REDs, 5α-reductase types 1 and 2; AR, androgen receptor; DHT, 5α-dihydrotestosterone; ER, estrogen receptor. (B) Structure of aromatase inhibitors used in this study. Androstenedione is a natural substrate of aromatase. Steroidal aromatase inhibitor, exemestane has an androstenedione-like structure.

clinical management of both primary and advanced breast cancer in postmenopausal women [5]. AIs are classified into two classes according to their modes of action. Type I AIs are steroidal inhibitions and one of them, exemestane (EXE) inhibits aromatase irreversibly and has an androstenedione (Δ_4)-like structure (Fig. 1B) [5–7]. Type II AIs are non-steroidal inhibitions and include aminoglutethimide (AGM), anastrozole, and letrozole [5].

Results of *in vivo* study using ovariectomized (OVX) rats demonstrated that EXE and its principal metabolite form, 17-hydroexemestane (17H-EXE) but not letrozole significantly prevented bone loss in OVX rats [8,9]. EXE and its principal metabolite, 17H-EXE, are structurally related to Δ_4 and bind to androgen receptor (AR) with relatively low affinity compared to 5α-dihydrotestosterone (DHT) [7]. These finding suggest that EXE may demonstrate protective effects toward bone tissues through its androgenic actions. However, detailed mechanisms of effects of EXE or androgen itself on human bone cells have remained largely unknown.

Various studies using human or animal bone tissues [10,11] and osteoblast cell culture using osteosarcoma cells [12,13] demonstrated that aromatase mRNA or protein was detected in osteoblast cells, which play an important role in bone remodeling. Therefore, in this study, we focused on effects of EXE in human osteoblast in an initial attempt to evaluate the effects of these AIs (summarized in Table 1 and Fig. 1B) [5–7,14], including AGM, EXE, and an experimental compound for inhibition of aromatase, Aromatase Inhibitor I (AI-I) [14] on human osteoblast and osteoblast-like cell lines. In our present study, we employed normal human cell line, hFOB, which maintains native characteristics of sex steroid hormone pathway of human osteoblasts, i.e., expression of AR, ERβ but not ERα, and aromatase. We also employed other osteoblast-like cell lines, Saos-2 and MG-63 which expressed ERα as well as ERβ in order to further study the mechanisms of effects of AI on human osteoblasts. We first examined the effects of estradiol (E2), DHT, progesterone (Prg), and AIs described above on cell proliferation of these cell lines, because the status of cell proliferation is important in the maintenance of homeostasis of bone tissue [15]. In addition, the effects of AIs on the conversion ratio of Δ_4 into E2 or testosterone (TST) in hFOB cultured medium were examined. We then screened E2, DHT, and EXE responsive genes using a microarray analysis in these cells, in order to further characterize the possible genomic effects of EXE on cell proliferation of osteoblasts. In this microarray analysis, hFOB was employed in order to examine the effects of E2, DHT, and EXE on native status of human osteoblasts but not on pathological status of osteoblasts such as osteosarcomas.

Materials and methods

Chemicals

Exemestane (EXE; FCE24304; 6-methyleneandrosta-1,4-diene-3,17-dione) and 17-hydroexemestane (17H-EXE; FCE25071; 6-methyleneandrosta-1,4-diene-17β-ol-3-one) were obtained from Pfizer, Inc. (MI, USA). Aminoglutethimide (AGM) and Aromatase Inhibitor I [AI-I; 4-(Imidazolylmethyl)-1-nitro-9*H*-9-xanthenone] were obtained from Sigma-Aldrich Co. (MO, USA) and EMD Biosciences, Inc. (CA, USA), respectively. Estradiol (E2), progesterone (Prg), and RU38,486 (RU; mifepristone), spironolactone were obtained from Sigma-Aldrich. ICI 182,780 (ICI; fulvestrant) and hydroxyflutamide (OHF) were obtained from Tocris Cookson Inc. (MO, USA) and Toronto Research Chemicals, Inc. (Ontario, Canada), respectively. 5α-dihydrotestosterone (DHT) was obtained from Wako Pure Chemical industries, Ltd. (Osaka, Japan).

Table 1
Aromatase inhibitors used in this study

	Aminoglutethimide	Exemestane	Aromatase inhibitor I
Trademark [a]	Cytadren®	Aromasin®	–
Type [b]	Type II	Type I	Type II
Generation	First	Third	–
IC50 (nM) [c]	3000	50	40

[a] Cytadren® is trademark of Novartis Pharmaseutical Corporation. Aromasin® is trademark of Pfizer Inc. Aromatase Inhibitor I is non-clinical compound of Calbiochem®.

[b] Type I is steroidal compound. Type II is a non-steroidal compound.

[c] Refs. Aminoglutethimide and Exemestane are Miller et al. [5]; Aromatase Inhibitor I is Recanatini et al. [14].

These materials were dissolved in pure ethanol (Wako Pure Chemical industries) and serially diluted (final concentrations: 10^{-12} M to 10^{-5} M), respectively. AGM was dissolved in DMSO (Wako Pure Chemical industries). The final concentration of ethanol and DMSO used in this study did not exceed 0.05%.

Osteoblast cell and osteoblast-like cell lines and culture conditions

Human normal osteoblast cell, hFOB 1.19 cell line (CRL-11372) was obtained from American Type Culture Collection (VA, USA). hFOB 1.19 cell was cultured according to the protocol previously described [16]. The cell line was maintained in a mixture of Dulbecco's Modified Eagle Medium and Ham's F12 medium (1:1) without phenol red (Invitrogen Corporation, CA, USA) supplemented with 10% fetal bovine serum (FBS; JRH Biosciences, KS, USA) and 50 mg/mL G 418 sulfate (EMD Biosciences). Human osteosarcoma cell lines Saos-2 and MG-63 were provided from the Cell Resource Center for Biomedical Research, Tohoku University (Sendai, Japan) and were maintained in a RPMI-1640 (Sigma-Aldrich) with 10% FBS. These cells were pre-incubated for 24 h with FBS-free medium prior to examination in order to remove exo-/endogenous steroid hormones from the culture medium and study the effects of various compounds in the absence of steroids and also to synchronize the cell cycle. Different concentrations of test compounds were added, and the assay was terminated after 3 or 5 days by removing the medium from wells. Steroid blockers were added simultaneously.

Characteristics of hFOB, Saos-2, and MG-63

Expressions of relevant steroid receptors, i.e., ERα, ERβ, and AR were determined using quantitative RT-PCR methods in hFOB, Saos-2, and MG-63 cell lines. mRNA transcripts of steroid synthesis/metabolite enzymes, aromatase, 17β-hydroxysteroid dehydrogenase (17β-HSD) types 1, 2, 3, 4, and 5, and 5α-reductase (5α-Red) types 1 and 2 were all evaluated using RT-PCR methods. The details of quantitative RT-PCR including primer sets employed were previously described in detail [17,18]. Positive controls for these receptors and enzymes were cell lines of human breast cancer, T-47D, and human prostate cancer, LNCaP obtained from Cell Resource Center for Biomedical Research, Tohoku University (Sendai, Japan). Alkaline phosphatase (ALP), an osteoblast-specific marker, was also studied using RT-PCR for characterization of these cell lines.

Estradiol and testosterone production assay

hFOB cells were plated in 10 mm dishes at a density of 10^6 viable cells and cultured for 48 h. Then media were changed to FBS-free medium, and hFOB cells were incubated with 10^{-7} M androstenedione (Δ_4; Sigma-Aldrich) in the presence or absence of EXE or AI-I (10^{-7} M). The media were then collected after 24 h, and E2 and TST were measured by solid-phase radioimmunoassay. Radioimmunoassay was performed in SRL Inc. (Tokyo, Japan) using DPC estradiol kit and DPC total testosterone kit (Diagnostic Products Corporation, LA, USA). In addition, we confirmed that the concentrations of E2 and TST were under the detection limits (E2, 5 pg/mL; TST, 30 pg/mL) in the serum- and phenol red-free medium.

Cell proliferation assay

hFOB, Saos-2, and MG-63 cells were treated with steroids and test compounds for 24, 48, and 72 h, when specimens were harvested and evaluated for cell proliferation using the WST-8 method (Cell Counting Kit-8; Dojindo Inc., Kumamoto, Japan) [18]. Optical densities (OD, 450 nm) were evaluated using a SpectraMax 190 microplate reader (Molecular Devices, Corp., CA, USA) and Softmax Pro 4.3 microplate analysis software (Molecular Devices). The status of proliferation (%) was calculated according to the following equation: (cell OD value after test materials treated / vehicle control cell OD value) × 100.

Alkaline phosphatase activity assay

hFOB, Saos-2, and MG-63 cells were plated in 48 well plate at a density of 10^6 viable cells and cultured for 48 h. All cell lines were treated with 10^{-9} to 10^{-7} M exemestane for 72 h, when cells were lysed with 0.05% Triton X-100 (Wako Pure Chemical industries) and evaluated for alkaline phosphatase activity

Table 2
Primer sequences used in quantitative RT-PCR analysis

cDNA	GB#	Sequence	cDNA position	Size (bp)
MYBL2	NM_002466	Forward 5′-GTAACAGCCTCACGCCCAAGA-3′ Reverse 5′-TCCAATGTGTCCTGTTTGTTCCA-3′	1522–1615	94
OSTM1	NM_014028	Forward 5′-TTGAGAATAAGGCTGAACCTGGAAC-3′ Reverse 5′-TTACAGGCACTGTGTCACTGCAAG-3′	801–926	126
HOXD11[a]	NM_021192	Forward 5′-CAC TGT CCT TGG GTT TAA TG-3′ Reverse 5′-GGT AAA ATT GTA ACG GGA CG-3′	1091–1245	174
GPC2	NM_152742	Forward 5′-AGA AAT GTG GTC AGC GAA GC-3′ Reverse 5′-ACA CCT TCG CAC TGT TTT CC-3′	871-1183	313
ADCYAP1R1	NM_001118	Forward 5′-CAG CAA AAG GGA AAG ACT CG-3′ Reverse 5′-GAG CTG CTC TTG CTC AGG AT-3′	1351–1584	234
COL1A1	NM_000088	Forward 5′-GGT GGT GGT TAT GAC TTT GGT T-3′ Reverse 5′-CTT GGC TGG GAT GTT TTC AGG T-3′	3784–4092	309
SMAD1[a]	NM_005900	Forward 5′-GGT TCA CCT CAT AAT CCT-3′ Reverse 5′-CCT TTG TCA GTT CTC AAT C-3′	1779–1887	127
SMAD5[a]	NM_005903	Forward 5′-AGC TAA AGC CGT TGG ATA-3′ Reverse 5′-AGG CAC TAA TAC TGG AGG T-3′	668–768	119
RUNX2	NM_004348	Forward 5′-GTG GAC GAG GCA AGA GTT T-3′ Reverse 5′-TAC TGG GAT GAG GAA TGC G-3′	782–961	198
SPARC	NM_003118	Forward 5′-CCT GTA CAC TGG CAG TTC-3′ Reverse 5′-CCA GGG CGA TGT ACT TGT C-3′	793–937	163
ALP	NM_000478	Forward 5′-ACC ATT CCC ACG TCT TCA CA-3′ Reverse 5′-AGA CAT TCT CTC GTT CAC CGC C-3′	1379–1540	162
RPL13A	NM_012423	Forward 5′-CCT GGA GGA GAA GAG GAA AGA GA-3′ Reverse 5′-TTG AGG ACC TCT GTG TAT TTG TCA A-3′	487–612	126

GB#, GeneBank accession number.
All primer sets were designed using OLIGO Primer Analysis Software (TAKARA Bio Inc., Shiga, Japan).
[a] Forward and reverse primers were located in sama exon.

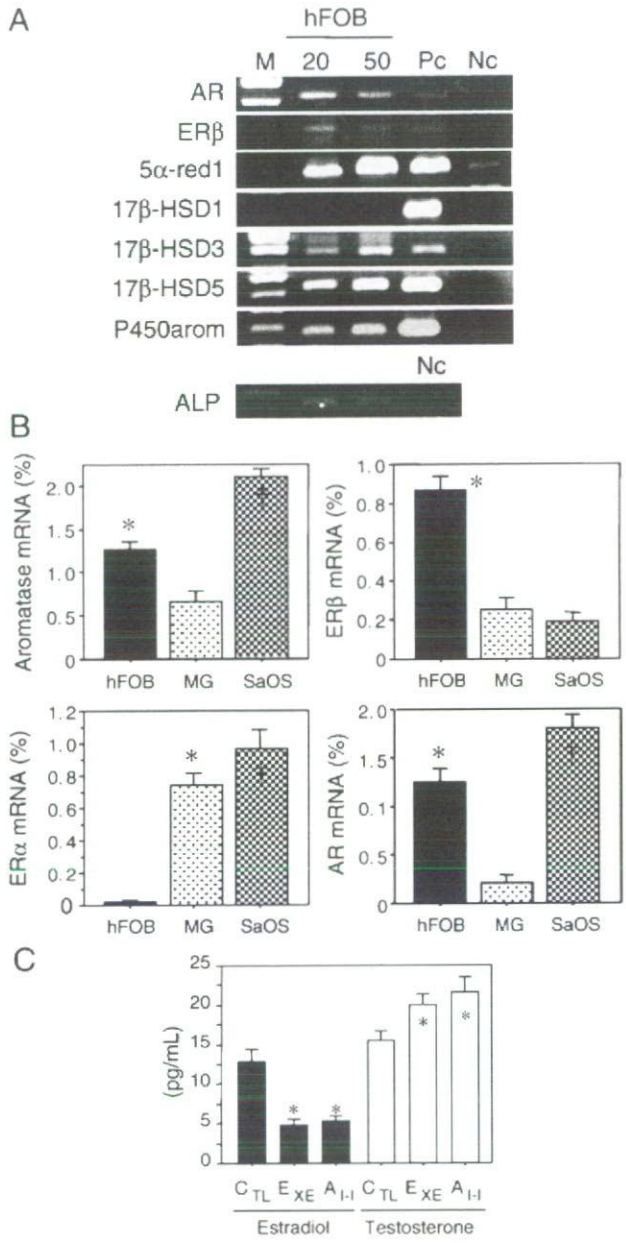

Fig. 2. (A) Results of RT-PCR analysis of steroid hormone receptors and steroid-related enzymes. Both 20 and 50 ng/μL cDNA of hFOB were used for PCR (ALP was 20 ng/μL alone). AR, androgen receptor; ER, estrogen receptor; 5α-red1, 5α-reductase type 1; 17β-HSD, 17β-hydroxysteroid dehydrogenase; P450 arom, aromatase; M, molecular marker; Pc, positive control; Nc, negative control. (B) Expression levels of aromatase, AR, ERα, and ERβ in hFOB, Saos-2, and MG-63. $*p<0.05$ vs. MG-63 (aromatase and AR), vs. MG-63 and vs. Saos-2 (ERβ), vs. hFOB (ERα); $^{\dagger}p<0.05$ vs. hFOB and MG-63 (aromatase and AR), vs. MG-63 and hFOB (ERα). (C) Estradiol and testosterone productions in hFOB cells. The data are expressed as the mean SD ($n=3$). $*p<0.05$ vs. control cells (CTL). EXE, 10^{-7} M exemestane; AI-I, 10^{-7} M aromatase inhibitor I.

using the *p*-nitrophenylphosphate method (LabAssay ALP; Wako Pure Chemical industries) [19]. Optical densities (OD, 405 nm) were evaluated using a SpectraMax 190 microplate reader (Molecular Devices) and Softmax Pro 4.3 microplate analysis software (Molecular Devices). ALP activity (units/μL)=(concentration of *p*-nitrophenol/15 min)×1 (dilution factor of sample). The ALP activities were presented as units/μL/10^6 cells. The ALP activity levels in each case were represented as a ratio of vehicle control (%).

Microarray analysis

The procedure was based on a previously reported study [20]. Cell lysates were prepared using RLT buffer (QIAGEN GmbH, Hilden, Germany). Total RNA was extracted using RNeasy Mini Kit (QIAGEN). First-strand cDNA was synthesized by incubating 5 μg of total RNA with 200 U SuperScript II reverse transcriptase (Invitrogen), 100 pmol T7-(dT)24 primer (Invitrogen). Ten units of T4 DNA polymerase (Invitrogen) were then added, and the dsDNA was mixed with T7 RNA polymerase (Invitrogen). The purified cRNA was fragmented at 300–500 bp as target solution. Hybridization was performed with the GeneChip Human Genome 133 ver. 2.0 (Affymetrix, Inc., CA, USA). The reacted arrays were then scanned as digital image files and scanned data were analyzed with GeneChip software (Affymetrix). Relative levels of gene expression were calculated by global normalization.

Data were subjected to hierarchical clustering analysis and visualization using the Cluster and TreeView programs (Stanford University) in order to generate tree structures based on the degree of similarity, as well as matrices comparing the levels of expression of individual genes in each sample [21].

Real-time PCR

Real-time PCR was carried out using the LightCycler System and the FastStart DNA Master SYBR Green I (Roche Diagnostics GmbH, Mannheim, Germany). The primer sequences used in this study are summarized in Table 2. An initial denaturing step of 95 °C for 10 min was followed by 35 cycles, respectively, at 95 °C for 10 min; 15 s annealing at 65 °C (ALP, COL1A1), 64 °C (MYBL2, OSTM1, RPL13A), 62 °C (SMAD1, SMAD5, SPARC, RUNX2), or 60 °C (HOXD11); and extension for 15 s at 72 °C. Negative control experiments included those lacking cDNA substrates to confirm the presence of exogenous contaminant DNA. No amplified products were detected under these conditions. The mRNA levels in each case were represented as a ratio of RPL13A (%) [22].

Immunohistochemistry of AR

Five non-pathological bone tissues were retrieved from surgical pathology files (two females and three males, 17 to 55 years old) of Department of Pathology, Tohoku University Hospital (Sendai, Japan).

Tissue sections were immunostained using a biotin-streptavidin method with Histofine kit (Nichirei Co. Ltd., Tokyo, Japan). The monoclonal antibody for AR (AR411) [23] was obtained from DakoCytomation (Kyoto, Japan). Experimental procedures employed in our present study have been previously described in detail [22,23]. The dilutions of primary AR antibody were 1:100. The antigen-antibody complex was then visualized with 3,3′-diaminobenzidine solution, and counterstained with hematoxylin. Prostate cancer was used as a positive control for AR. Normal mouse IgG was used as a negative control for immunostaining and no specific immunoreactivity was detected.

Statistical analysis

Results were expressed as mean±SD. Statistical analysis was performed with the StatView 5.0 J software (SAS Institute Inc., NC, USA). All data were analyzed by analysis of variance (ANOVA) followed by post hoc Bonferroni/Dunnett multiple comparison test. A p-value<0.05 was considered to indicate statistical significance.

Results

Characteristics of hFOB, MG-63, and Saos-2 cell line

Characteristics of osteoblast and osteoblast-like cell lines are summarized in Figs. 2A and B. hFOB cells expressed mRNA transcripts of AR and ERβ. Relatively low level of ERα mRNA transcript was detected in hFOB cells. Aromatase, 17β-HSD type 1, 3, and 5, and 5α-Red types 1 and 2 mRNA transcripts were all detected in hFOB cells by

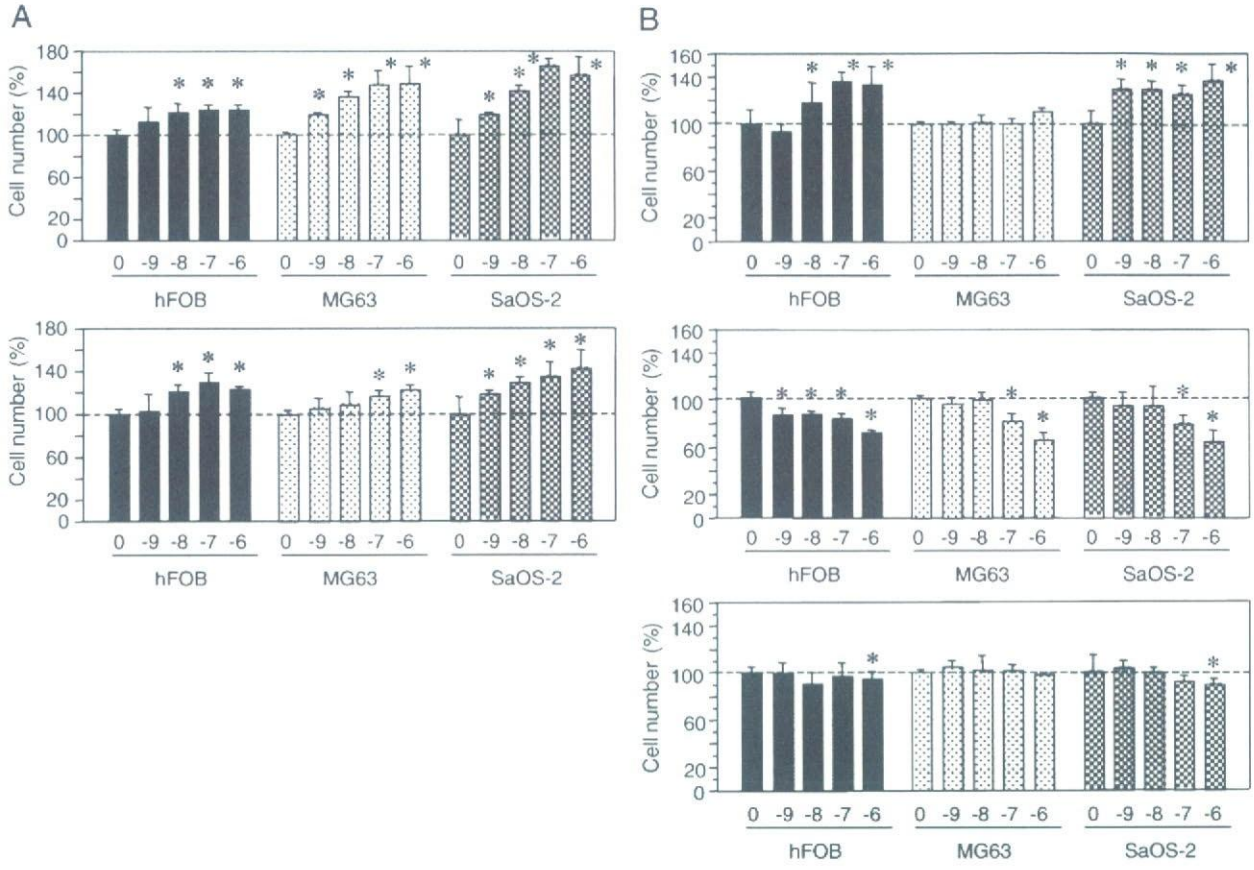

Fig. 3. (A) Proliferation of hFOB cells treated by estradiol (top) and 5α-DHT (bottom). *$p<0.05$ vs. vehicle control (0). (B) Proliferation of hFOB cells treated by exemestane (top), aminogluthetimide (middle), and Aromatase Inhibitor-I (bottom). *$p<0.05$ vs. vehicle control (0). $n=5$.

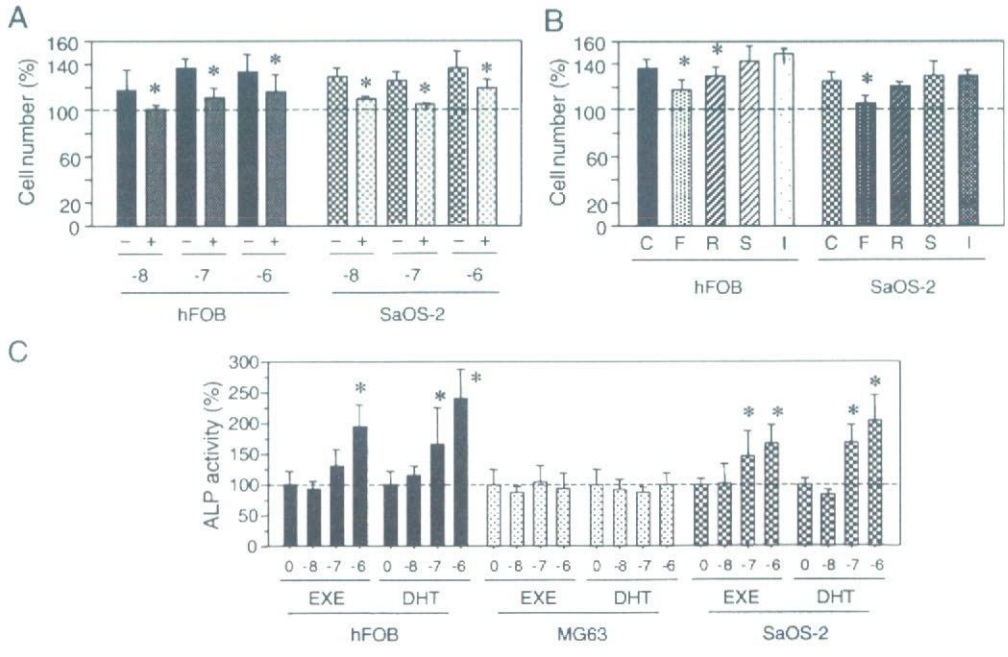

Fig. 4. (A) Effects of hydroxyflutamide on exemestane (10^{-8} to 10^{-6} M) stimulated the cell proliferation of both hFOB and Saos-2. With (+) or without (−) hydroxyflutamide, $p<0.05$ vs. without hydroxyflutamide (*). (B) Effects of steroid receptor blockers on exemestane (10^{-7} M) stimulated cell proliferation of hFOB and Saos-2. C, 10^{-7} M exemestane; F, hydroxyflutamide (5×10^{-6} M); R, RU38,486 (5×10^{-6} M); S, spironolactone (5×10^{-6} M); I, ICI182,720 (5×10^{-6} M). *$p<0.05$ vs. C (C) ALP activity in hFOB, Saos-2, MG-63 treated with exemestane (EXE, 10^{-8} to 10^{-6} M), or 5α-DHT (DHT, 10^{-8} to 10^{-6} M). *$p<0.05$ vs. vehicle control (0).

RT-PCR. Aromatase, ERα, ERβ, and AR were all detected in osteoblast-like cell lines, Saos-2 and MG-63 (Fig. 2B). In hFOB cell, expression of ERβ mRNA was more predominant than that of ERα mRNA. ERα mRNA as well as ERβ mRNA was detected in Saos-2 and MG-63 cells. The levels of AR mRNA expression in both hFOB and Saos-2 were significantly higher ($p=0.01$) than that in MG-63. ALP mRNA was also detected in intact hFOB, Saos-2, and MG-63 cells (data not present), respectively.

Estradiol and testosterone production

Results were summarized in Fig. 2C. The E2 levels in the medium of hFOB supplemented with Δ_4 treated with EXE or AI-I were significantly lower than that of cells without AIs. The levels of TST in the medium of hFOB supplemented with Δ4 treated with EXE or AI-I were significantly higher than that of cells without AIs.

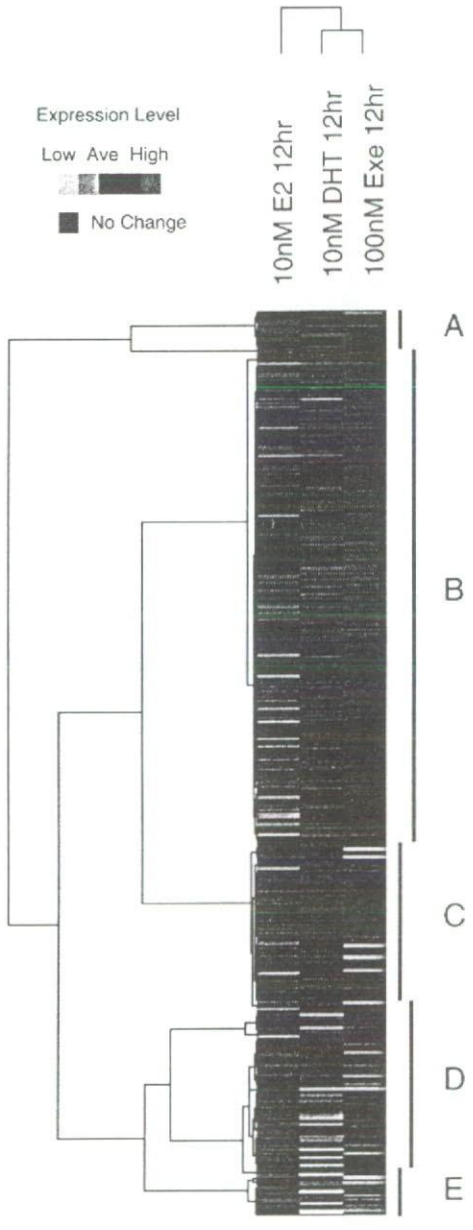

Fig. 5. In clustering analysis of the expression levels of each gene in hFOB cells treated with estradiol (E2), 5α-dihydrotestosterone (DHT), and exemestane (Exe).

Cell proliferation

Results of the cell proliferation assays are summarized in Figs. 3 and 4. There was a significant increment in the number of the cells after 72 h in hFOB, Saos-2, and MG-63 cells treated with 10^{-9} M (Saos-2 and MG-63) or 10^{-8} M (hFOB) to 10^{-6} M E2 (Fig. 3A). The cell number of hFOB and Saos-2 cells treated by 10^{-9} M (Saos-2) or 10^{-8} M (hFOB) to 10^{-6} DHT for 72 h was also significantly higher than control (Fig. 3A). The number of MG-63 cells was significantly increased only by high dose of DHT (10^{-7} M and 10^{-6} M) treatments (Fig. 3A). Prg (10^{-9} M to 10^{-6} M) treatments did not change the number of cells even after 72 h in all three cell lines examined (data not present).

Both EXE (Fig. 3B) and 17H-EXE (data not present) treatments of 10^{-8} M to 10^{-6} M, which were comparable to pharmacological inhibition doses of aromatization (Table 1), significantly increased the hFOB cell number for 72 h, respectively. In Saos-2 cells treated with relatively low dose, 10^{-9} to 10^{-6} M EXE, there was a significant increment in the number of the cells after 72 h (Fig. 3B). However, all the dose (10^{-9} M to 10^{-6} M) of EXE employed did not results in the change of cell number of MG-63 even after 72 h of treatment (Fig. 3B). The cell number of both hFOB and Saos-2 cells treated by both 10^{-6} M EXE and/or 17H-EXE for 48 h was also significantly higher than that treated for 24 h (data not present).

AGM treatment [10^{-9} (hFOB) or 10^{-7} (Saos-2 and MG-63) to 10^{-6} M] diminished the number of these three cells (Fig. 3B) and morphological changes in these cells were consistent with those caused by cytotoxic effects (data not present). AI-I treatment (10^{-9} to 10^{-7} M) was not associated with significant increment of the cell number in these cell lines (Fig. 3B). Only high dose (10^{-6} M) of AI-I significantly diminished the cell numbers of hFOB and Saos-2 but not of MG-63 (Fig. 3B).

The androgen receptor antagonist OHF (5×10^{-6} M) diminished the effects of EXE on these increments of both hFOB and Saos-2 cells (Figs. 4A and B). Treatment with RU but not spironolactone and ICI also inhibited EXE effects on hFOB cells (Fig. 4B).

ALP activity assay

Results of the ALP activity assay were summarized in Fig. 4C. There was a significant increment in the ALP activity of both hFOB and Saos-2 cells treated with 10^{-7} M (Saos-2) and/or 10^{-6} M (hFOB and Saos-2) EXE. Both 10^{-7} M and 10^{-6} M DHT treatment also increased the ALP activity in hFOB and Saos-2 cells, respectively. There were no changes of ALP activity in MG-63 treated with 10^{-8} M to 10^{-6} M of EXE and DHT, respectively.